Hindawi Publishing Corporation
ISRN Power Engineering
Volume 2013, Article ID 517940, 30 pages
http://dx.doi.org/10.1155/2013/517940

Review Article

Broadband over Power Lines Systems Convergence: Multiple-Input Multiple-Output Communications Analysis of Overhead and Underground Low-Voltage and Medium-Voltage BPL Networks

Athanasios G. Lazaropoulos

School of Electrical and Computer Engineering, National Technical University of Athens, 9 Iroon Polytechniou Street, Zografou, 15780 Athens, Greece

Correspondence should be addressed to Athanasios G. Lazaropoulos; aglazaropoulos@gmail.com

Received 26 April 2013; Accepted 6 June 2013

Academic Editors: V. Fernao Pires and W. Jaikla

This review paper reveals the broadband potential of overhead and underground low-voltage (LV) and medium-voltage (MV) broadband over power lines (BPL) networks associated with multiple-input multiple-output (MIMO) technology. The contribution of this review paper is fourfold. First, the unified value decomposition (UVD) modal analysis is introduced. UVD modal analysis is a new technique that unifies eigenvalue decomposition (EVD) and singular value decomposition (SVD) modal analyses achieving the common handling of traditional SISO/BPL and upcoming MIMO/BPL systems. The validity of UVD modal analysis is examined by comparing its simulation results with those of other exact analytical models. Second, based on the proposed UVD modal analysis, the MIMO channels of overhead and underground LV and MV BPL networks (distribution BPL networks) are investigated with regard to their inherent characteristics. Towards that direction, an extended collection of well-validated metrics from the communications literature, such as channel attenuation, average channel gain (ACG), root-mean-square delay spread (RMS-DS), coherence bandwidth (CB), cumulative capacity, capacity complementary cumulative distribution function (CCDF), and capacity gain (GC), is first applied in overhead and underground MIMO/LV and MIMO/MV BPL channels and systems. It is found that the results of the aforementioned metrics portfolio depend drastically on the frequency, the power grid type (either overhead or underground, either LV or MV), the MIMO scheme configuration properties, the MTL configuration, the physical properties of the cables used, the end-to-end distance, and the number, the electrical length, and the terminations of the branches encountered along the end-to-end BPL signal propagation. Third, three interesting findings concerning the statistical properties of MIMO channels of distribution BPL networks are demonstrated, namely, (i) the ACG, RMS-DS, and cumulative capacity lognormal distributions; (ii) the correlation between RMS-DS and ACG; and (iii) the correlation between RMS-DS and CB. By fitting the numerical results, unified regression distributions appropriate for MIMO/BPL channels and systems are proposed. These three fundamental properties can play significant role in the evaluation of recently proposed statistical channel models for various BPL systems. Fourth, the potential of transformation of overhead and underground LV/BPL and MV/BPL distribution grids to an alternative solution to fiber-to-the-building (FTTB) technology is first revealed. By examining the capacity characteristics of various MIMO scheme configurations and by comparing these capacity results against SISO ones, a new promising urban backbone network seems to be born in a smart grid (SG) environment.

1. Introduction

The distribution power grids—that is, overhead and underground low-voltage (LV) and medium-voltage (MV) networks—can become the key to delivering broadband last-mile access in remote and/or underdeveloped areas and simultaneously to the development of an advanced IP-based power system [1–6]. This power grid upgrade can be achieved

through the deployment of broadband over power lines (BPL) networks [7–14].

Despite their great broadband promises, distribution power grids constitute a rather hostile medium for communications signal transmission. Attenuation, multipath due to various reflections, noise, and electromagnetic interference are the main problematic issues [15–22]. Since overhead and underground LV/BPL and MV/BPL channels mix the nasty behavior of a power line with that of a communication channel, each of the aforementioned adverse factors significantly degrades the overall performance of BPL networks [23–25].

Recently, new interest arises due to developments regarding multiple-input multiple-output (MIMO) transmission scheme configurations for BPL networks and BPL coexistence with other broadband technologies [13, 14, 26–30]. Actually, the need of coexistence among overhead and underground LV/BPL and MV/BPL networks (intraoperability) will be a necessary prerequisite before investigating the cooperative communications between distribution BPL networks and other broadband technologies (interoperability) [28, 31–38]. Despite the urgent demand for systems intraoperability/interoperability, today's distribution BPL network capacity performance seems significantly worse than that of other competitive broadband technologies—wired, such as fiber and DSL, and wireless, such as Wi-Fi and WiMAX. Hence, there is a need of not only utilizing existing technical developments, but also inventing and exploiting novel ones such as MIMO technology.

Being prominent from the wireless world [38–46] and recently applied in various BPL networks [13, 14, 33, 47–56], the potential of integrating MIMO technology with distribution BPL networks is investigated. Towards that direction, MIMO capabilities of distribution BPL networks are compared with today's single-input single-output (SISO) ones either in transmission or in spectral efficiency fields.

For efficient MIMO/BPL (either MIMO/LV/BPL or MIMO/MV/BPL) communications, a thorough understanding of the MIMO signal transmission at high frequencies along the overhead and underground LV and MV power lines is required. To facilitate MIMO analysis, the hybrid model that is usually employed to examine the behavior of BPL transmission channels installed on multiconductor transmission line (MTL) structures is also used in this review paper [2, 3, 5, 6, 9, 10, 12–14]. This hybrid method, based on a combination of bottom-up [57–65] and top-down [8, 15, 18, 24, 58, 62, 64, 66–69] approaches, receives as inputs accurately determined parameters, such as the MIMO scheme implementation, the power grid type (either overhead or underground, either LV or MV), the MTL configuration, the physical properties of cables, and the grid topology, and delivers as outputs accurate results in terms of channel attenuation. Actually, exploiting the acquired MIMO/BPL knowledge of [13, 14], MIMO expansion of the hybrid method is first presented in order to (i) achieve a smooth expansion of SISO to MIMO analysis and (ii) unify eigenvalue decomposition (EVD) and singular value decomposition (SVD) modal analyses under the aegis of the proposed unified value decomposition (UVD) modal analysis.

Based on the outputs of UVD modal analysis, broadband transmission characteristics, statistical performance metrics, and capacity measures are investigated through numerical results concerning simulated overhead and underground MIMO/LV/BPL and MIMO/MV/BPL networks [57, 62, 64, 67, 70]. The numerical results of UVD modal analysis are validated against already verified results of the accurate TM2 method, which are analytically presented in [13, 14].

More specifically, a set of important statistical performance metrics, such as the average channel attenuation, the average channel gain (ACG), the root-mean-square delay spread (RMS-DS), and the coherence bandwidth (CB), tries to elicit the common and the different aspects of overhead and underground MIMO/LV/BPL and MIMO/MV/BPL channels. In addition, two fundamental properties of several wireline channels (e.g., DSL, coaxial, and phone links) are first validated in overhead and underground MIMO/LV/BPL and MIMO/MV/BPL systems; namely, (i) ACG and RMS-DS are negatively correlated lognormal random variables being in agreement with recently proposed statistical BPL channel models [71–79]. A new approximation—UN1 approach—suitable for the design of overhead and underground MIMO/BPL channels is proposed and compared to existing distributions; and (ii) CB and RMS-DS correlation behavior can be described by hyperbolic functions. By fitting the simulation results, a new approximation—UN2 approach—appropriate for MIMO/BPL channels is proposed [78–82]. Moreover, lognormal distributions for the cumulative distribution functions (CDFs) of ACG, RMS-DS, and cumulative capacity—suitable for overhead and underground MIMO/LV/BPL and MIMO/MV/BPL channels—are used so as to (a) be imposed by design in the upcoming BPL statistical channel modeling and (b) operate as evaluation measures of the statistical channel models proposed [71–73, 76–79].

Apart from statistical performance metrics, suitable capacity metrics, such as the cumulative capacity, the capacity complementary cumulative distribution functions (capacity CCDF), and the capacity gain (GC) of MIMO/BPL systems, are applied. It is unveiled that MIMO/BPL systems can define an alternative technological solution to the existing fiber-optic technology and especially to the fiber-to-the-building (FTTB) systems. Depending on BPL system investment budget, technoeconomic and socioeconomic characteristics, required system complexity, power grid type, power grid topology, IPSDM limits applied, operation frequency band, and BPL intraoperability/interoperability requirements, different single- and multiport implementations may be applied in improving today's system capacities. By fully exploiting the MIMO technology, the increase of the capacity of both overhead and underground MIMO/LV/BPL and MIMO/MV/BPL systems is notable exceeding 8 Gbps. Using only the existing infrastructure and electromagnetic compatibility limits, the imminent MIMO/BPL technology implementations promise better capacity results by a factor of up to 3.65 in comparison with the best today's capacity results for given power grid type and power grid topology. Hence, the forthcoming MIMO/BPL capacity boost indicates that the BPL technology should be examined as (i) an emerging

urban backbone network and (ii) a promise towards BPL intraoperability/interoperability.

The rest of this review paper is organized as follows. In Section 2, the overhead and underground LV and MV configurations adopted in this paper are presented. Section 3 introduces the MTL theory and modal analysis along with the necessary assumptions concerning BPL transmission. Apart from the presentation of EVD and SVD modal analyses, the UVD modal analysis is highlighted in order to realize the necessary upgrade from SISO/BPL to MIMO/BPL consideration. Section 4 details the statistical performance metrics and the capacity measures applied in this review paper for the upcoming MIMO/BPL analysis. In Section 5, a series of numerical results and conclusions is provided, aiming at marking out how the various features of the overhead and underground MIMO/LV and MIMO/MV channels and systems influence BPL transmission, statistical performance metrics, and capacity measures. On the basis of the confirmed fundamental properties, new regression approximations are proposed. Moreover, after providing the SISO capacity of overhead and underground LV/BPL and MV/BPL channels and systems, different MIMO scheme configurations are demonstrated and compared regarding their suitability and performance for various overhead and underground LV/BPL and MV/BPL systems. A thorough MIMO scheme configuration investigation reveals the great capacity potential of overhead and underground MIMO/LV/BPL and MIMO/MV/BPL distribution power networks. Section 6 concludes this review paper.

2. The Physical BPL Layer

The overhead and underground LV and MV MTL configurations as well as the ground properties used across the following MIMO/BPL system analysis are outlined in this section [8, 15, 17, 23, 57, 59–61, 66, 67, 83–86].

2.1. Overhead LV and MV Power Distribution Networks. A typical case of overhead LV distribution line is depicted in Figure 1(a). Four parallel noninsulated conductors are suspended one above the other spaced by Δ_{LV} and located at heights h_{LV} above ground for the lowest conductor. The upper conductor is the neutral, while the lower three conductors are the three phases. This three-phase four-conductor ($n = 4$) overhead LV distribution line configuration is considered in the present work consisting of ASTER conductors. The exact dimensions for the overhead LV MTL configuration are detailed in [60, 61, 83–85, 87].

Overhead MV distribution lines hang at typical heights h_{MV}. Typically, three parallel noninsulated phase conductors spaced by Δ_{MV} are used above lossy ground. This three-phase three-conductor ($n = 3$) overhead MV distribution line configuration is considered in the present work consisting of ACSR conductors—see Figure 1(b). The exact properties of the overhead MV MTL configuration are detailed in [15, 16, 57, 67, 83, 86, 87].

2.2. Underground LV and MV Power Distribution Network. The underground LV distribution line that will be examined in the simulations is the three-phase four-conductor ($n = 4$) core-type YJV XLPE underground LV distribution cable buried 1 m inside the ground. The layout of this cable is depicted in Figure 1(c). The cable arrangement consists of the three-phase three-core-type conductors, one core-type neutral conductor, and one shield conductor. The shield is grounded at both ends. The exact dimensions of this underground LV MTL configuration are reported in [58, 59, 62, 63, 83, 84, 87, 88].

The underground MV distribution line that will be examined is the three-phase three-conductor ($n = 3$) sector-type PILC 8/10 kV distribution-class cable buried 1 m inside the ground [15–18, 89, 90]. The cable arrangement consists of the three-phase three-sector-type conductors, one shield conductor, and one armor conductor—see Figure 1(d). The shield and the armor are grounded at both ends. The underground MV MTL configuration specifications are detailed in [17, 91–94].

As it concerns BPL signal propagation in underground MTL configurations, due to the common practice of grounding at both ends, the shield acts as a ground return path and as a reference conductor. Hence, the inner conductors are separated electrostatically and magnetostatically from the remaining set. On the basis of this separation, the analysis may be focused only on the remaining five- or four-conductor transmission line (TL) of interest for underground LV—that is, the three phases, the neutral conductor, and the shield conductor—or MV configurations—that is, the three phases and the shield conductor, respectively. Repeatedly applied in [17, 58, 59, 62, 63, 66, 83, 87, 91–98], this is the common procedure either in theoretical analyses or in measurements.

2.3. Ground Properties. The properties of the ground are assumed common either in overhead or in underground BPL configurations. In detail, the conductivity of the ground is assumed $\sigma_g = 5$ mS/m and its relative permittivity $\varepsilon_{\mathrm{rg}} = 13$. In accordance with [15–17, 57–59, 62, 63, 67, 95, 99–102], these ground properties are suitable for the BPL signal propagation analysis at high frequencies (from 1 MHz to approximately 100 MHz) either in overhead or in underground BPL systems.

3. Modal Analysis of Overhead and Underground LV/BPL and MV/BPL Systems

In this section, through a matrix approach, the standard TL analysis is extended to the MTL case, which involves more than two conductors. First, a brief introduction to MTL theory is provided, which is accompanied with the necessary assumptions concerning BPL transmission via the entire distribution power grid. Second, a detailed modal analysis of overhead and underground LV/BPL and MV/BPL systems is highlighted; in particular, UVD modal analysis is proposed in order to (i) unify EVD and SVD modal analyses; (ii) describe the analysis convergence of SISO/BPL and MIMO/BPL configurations; and (iii) suggest appropriate methodology for the performance and capacity study of MIMO/BPL systems.

3.1. MTL Theory of Overhead and Underground LV/BPL and MV/BPL Systems. Signal transmission via overhead power

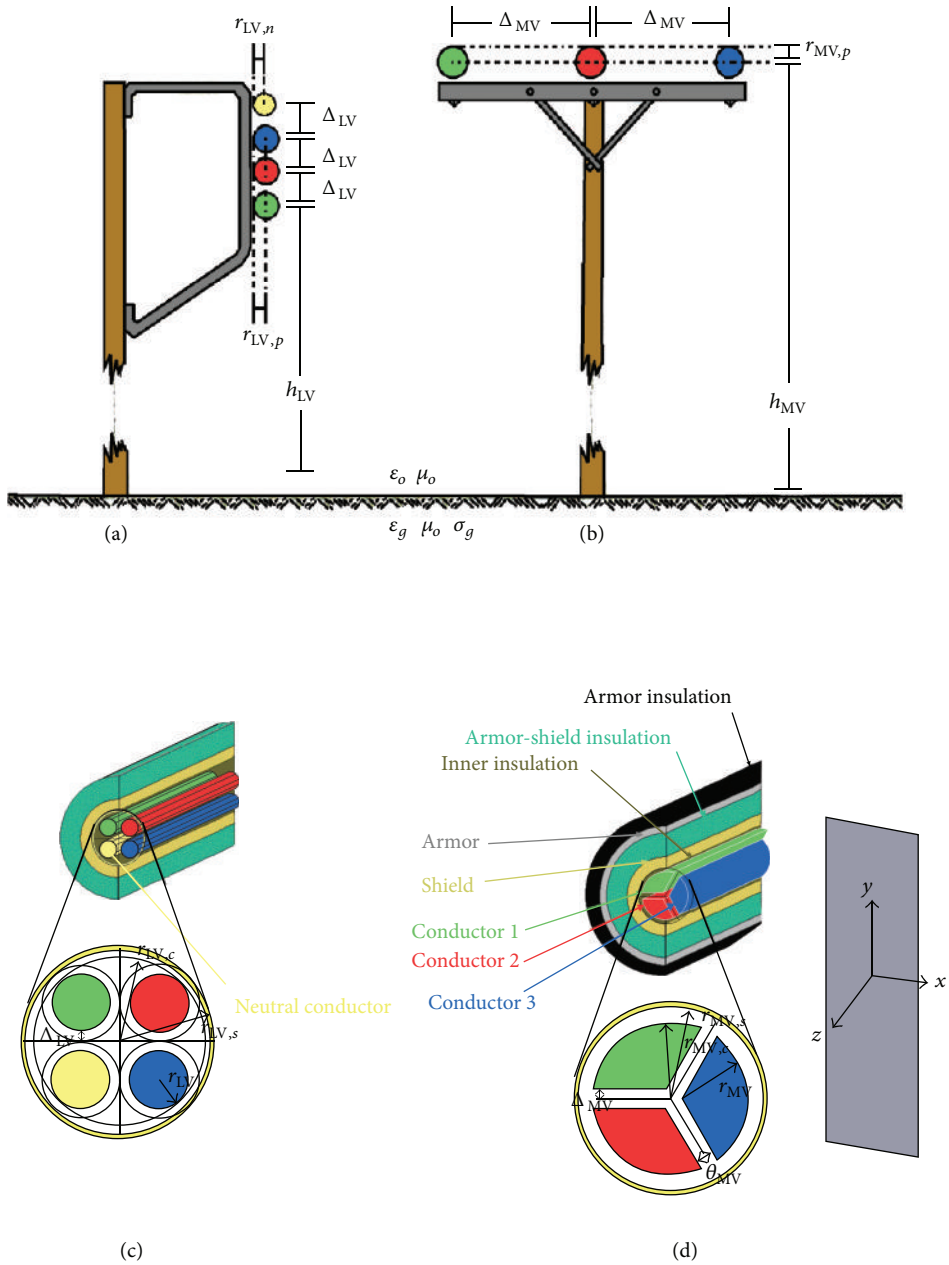

FIGURE 1: Typical multiconductor structures [15, 17, 58, 95]. (a) Overhead LV. (b) Overhead MV. (c) Underground LV. (d) Underground MV.

lines has been analyzed in [17, 58, 59, 62, 63, 95, 99–102], whereas signal transmission via three-phase underground power lines has been detailed in [17, 58, 59, 62, 63, 95, 99–102]. These formulations have the advantage that, contrary to other available models for overhead and underground power lines [85, 103–105], they are appropriate for broadband applications of overhead LV/BPL and MV/BPL systems.

Already described in [15, 17, 31, 56, 57, 60, 61, 67], compared to a two-conductor line supporting one forward- and one backward-traveling wave, an MTL structure with $n + 1$ conductors parallel to the z axis as depicted in Figures 1(a)–1(d) may support n pairs of forward- and backward-traveling waves with corresponding propagation constants. These waves may be described by a coupled set of $2n$ first-order partial differential equations relating the line voltages $V_i(z,t)$, $i = 1,\ldots,n$, to the line currents $I_i(z,t)$, $i = 1,\ldots,n$. Each pair of forward- and backward-traveling waves is referred to as a mode and presents its own propagation constant.

According to TM1 method—detailed in [15, 16, 57, 58, 65, 106] and briefly presented in Section 3.2—these modes may be examined separately across the overall overhead or underground LV or MV power distribution network under the following two assumptions.

(A1) The branching cables are assumed to be identical to the distribution cables. Hence, cables with identical modes are used throughout the network ensuring

that the mode propagation constants of all the cable segments are the same.

(A2) The termination points are assumed to be either ideal matches—achieved using adaptive modal impedance matching [107, 108]—or open circuit terminations. Hence, these termination points behave independently of frequency. Due to this frequency-independent nature of terminations, the branches and termination points are perfectly balanced ensuring that no mode mixing occurs anywhere in the network.

These two assumptions are general and consider BPL transmission regardless of the power grid type (either overhead or underground, either LV or MV) and MIMO scheme configuration. Because of the above assumptions, the n modes supported by the BPL configurations are completely separate giving rise to n independent transmission channels which simultaneously carry BPL signals [15–18, 57, 58, 65, 91, 106].

3.2. UVD Modal Analysis of Overhead and Underground LV/BPL and MV/BPL Systems. Since the number of transmit ports n_T and receive ports n_R in MIMO systems is not always equal, existing EVD modal analysis for SISO/BPL networks needs to be integrated with SVD modal analysis for MIMO communications networks so as to permit the general study of MIMO/BPL systems [39, 40, 48, 49, 52].

Taking advantage of the simplicity of TM1 method, UVD modal analysis is the technique that perceives the modular consideration of EVD and SVD modal analyses, concatenates them, and achieves the common handling of traditional SISO/BPL and upcoming MIMO/BPL systems. Based on EVD and SVD modal transfer functions, UVD modal analysis computes the extended channel transfer functions and various performance and capacity metrics imperative for the following MIMO/BPL analysis—further details concerning the metrics are provided in Section 4.

More specifically, the EVD modal voltages $\mathbf{V}^m(z) = \left[V_1^m(z) \ \cdots \ V_n^m(z)\right]^T$ and the EVD modal currents $\mathbf{I}^m(z) = \left[I_1^m(z) \ \cdots \ I_n^m(z)\right]^T$ may be related to the respective EVD line quantities $\mathbf{V}(z) = \left[V_1(z) \ \cdots \ V_n(z)\right]^T$ and $\mathbf{I}(z) = \left[I_1(z) \ \cdots \ I_n(z)\right]^T$ via the EVD transformations [15–18, 58, 60, 61]:

$$\mathbf{V}(z) = \mathbf{T}_V \cdot \mathbf{V}^m(z), \tag{1}$$

$$\mathbf{I}(z) = \mathbf{T}_I \cdot \mathbf{I}^m(z), \tag{2}$$

where $[\cdot]^T$ denotes the transpose of a matrix, $\mathbf{T}_V$ and $\mathbf{T}_I$ are $n \times n$ matrices depending on the frequency, the power grid type, the physical properties of the cables, and the geometry of the MTL configuration [15, 17, 58, 60, 61].

The TM1 method—based on the scattering matrix theory [15, 18, 19, 68, 69] and presented analytically in [18]—models the spectral relationship between $V_i^m(z)$, $i = 1, \ldots, n$, and $V_i^m(0)$, $i = 1, \ldots, n$, introducing operators $H_i^m\{\cdot\}$, $i = 1, \ldots, n$ so that

$$\mathbf{V}^m(z) = \mathbf{H}^m\left\{\mathbf{V}^m(0)\right\}, \tag{3}$$

where

$$\mathbf{H}^m\{\cdot\} = \operatorname{diag}\left\{H_1^m\{\cdot\} \ \cdots \ H_n^m\{\cdot\}\right\} \tag{4}$$

is a diagonal matrix operator whose elements $H_i^m\{\cdot\}$, $i = 1, \ldots, n$, are the EVD modal transfer functions [15–18].

Combining (1) and (4), the $n \times n$ channel transfer function matrix $\mathbf{H}\{\cdot\}$ relating $\mathbf{V}(z)$ with $\mathbf{V}(0)$ through

$$\mathbf{V}(z) = \mathbf{H}\left\{\mathbf{V}(0)\right\} \tag{5}$$

is determined from

$$\mathbf{H}\{\cdot\} = \mathbf{T}_V \cdot \mathbf{H}^m\{\cdot\} \cdot \mathbf{T}_V^{-1}. \tag{6}$$

Based on (4) and (6), the $n \times n$ channel transfer function matrix $\mathbf{H}\{\cdot\}$ of the overhead and underground SISO/LV/BPL and SISO/MV/BPL distribution networks is determined.

Based on (5), at the transmitting end side of the overhead and underground LV/BPL and MV/BPL distribution networks, n independent transmit ports—that is, $V_i(0)$, $i = 1, \ldots, n$—which share the same return reference conductor, can be used. At the receiving end side, due to coupling effects that provide interactions between different ports, n independent receive ports are available—that is, $V_i(z)$, $i = 1, \ldots, n$. Consequently, the $n \times n$ channel transfer function matrix $\mathbf{H}\{\cdot\}$, which is presented in (5) and (6), can describe multiport communications systems with n_T ($n_T \leq n$) transmit and n_R ($n_R \leq n$) receive ports. This multiport communications system is referred to as $n_T \times n_R$ MIMO/BPL system [13, 14, 31, 56, 76, 79]. During the following analysis, it is assumed that N_T and N_R are the active transmit port and the active receive port set, respectively, hereafter.

As it concerns the characterization of channels of the upcoming MIMO/BPL systems, from (6), the elements $H_{ij}\{\cdot\}$, $i, j = 1, \ldots, n$, of channel transfer function matrix $\mathbf{H}\{\cdot\}$ with $i = j$ are the cochannel (CC) transfer functions, while those with $i \neq j$ are the cross-channel (XC) transfer functions where H_{ij}, $i, j = 1, \ldots, n$, denotes the element of matrix $\mathbf{H}\{\cdot\}$ in row i of column j. Altogether, $H_{ij}\{\cdot\}$, $i, j = 1, \ldots, n$, are the transfer functions of MIMO channels (either CCs or XCs).

On the basis of the previous channel characterization, it is clear that the analysis concerning $n_T \times n_R$ MIMO/BPL systems is sustained on the generalization of the analysis concerning MIMO channels of a full $n \times n$ MIMO/BPL system—that is, all the available transmit and receive ports are active, either 4×4 MIMO/LV/BPL or 3×3 MIMO/MV/BPL—via the proposed UVD modal analysis. As shown in the following analysis, theUVD modal analysis permits the study of full $n \times n$ MIMO/BPL and SISO/BPL systems as case studies of a general $n_T \times n_R$ MIMO/BPL system [39, 40, 49, 52].

More specifically, based on the above definition of the EVD line voltages, the associated UVD transmit vector $\mathbf{V}^+(0) = \left[V_1^+(0) \ \cdots \ V_n^+(0)\right]^T$ is related to the EVD line voltages vector $\mathbf{V}(0)$ through a simple matrix relationship of the form

$$\mathbf{V}(0) = \mathbf{D}_V^{N_T} \cdot \mathbf{V}^+(0), \tag{7}$$

where $\mathbf{D}_V^{N_T}$ is the $n \times n$ UVD transmit voltage matrix with zero elements except in row j of column j where the value

is equal to 1 when transmit port j belongs to the set N_T. For example, in the case of full $n \times n$ MIMO/BPL and SISO/BPL systems, $\mathbf{D}_V^{N_T}$ is equal to $n \times n$ identity matrix and $n \times n$ matrix with only one 1 on the diagonal at the position of the active transmit port, respectively. Likewise, the UVD receive vector $\mathbf{V}^+(z) = \left[V_1^+(z) \ \cdots \ V_n^+(z)\right]^T$ can be related to the EVD line voltages vector $\mathbf{V}(z)$ through a similar matrix relationship

$$\mathbf{V}^+(z) = \mathbf{D}_V^{N_R} \cdot \mathbf{V}(z), \tag{8}$$

where $\mathbf{D}_V^{N_R}$ is the $n \times n$ UVD receive voltage matrix with zero elements except in row i of column i where the value is equal to 1 when receive port i belongs to the set N_R. For example, in the case of full $n \times n$ MIMO/BPL and SISO/BPL systems, $\mathbf{D}_V^{N_R}$ is equal to the $n \times n$ identity matrix and the $n \times n$ matrix with only one 1 on the diagonal at the position of the active receive port, respectively. Combining (5), (7), and (8), the $n \times n$ extended channel transfer function matrix $\mathbf{H}^+\{\cdot\}$ is determined from

$$\mathbf{H}^+\{\cdot\} = \mathbf{D}_V^{N_R} \cdot \mathbf{H}\{\cdot\} \cdot \mathbf{D}_V^{N_T}. \tag{9}$$

Apart from the insertion of $\mathbf{D}_V^{N_T}$ and $\mathbf{D}_V^{N_R}$, UVD modal analysis achieves the MIMO channel analysis generalization by exploiting both already existing EVD and SVD modal analyses [13, 14].

More specifically, adopting SVD modal analysis presented in [13, 14, 39, 40, 49, 52], the $n \times n$ extended channel transfer function matrix $\mathbf{H}^+\{\cdot\}$ can be decomposed into $\min\{n_T, n_R\}$ parallel and independent SISO channels where $\min\{x, y\}$ returns the smallest value between x and y. Then, the SVD modal transfer function matrix operator is given by

$$\begin{aligned}\widehat{\mathbf{H}}^m\{\cdot\} &= \widehat{\mathbf{T}}_V^H \cdot \mathbf{H}^+\{\cdot\} \cdot \widehat{\mathbf{T}}_I \\ &= \left(\widehat{\mathbf{T}}_V^H \cdot \mathbf{D}_V^{N_R} \cdot \mathbf{T}_V\right) \cdot \mathbf{H}^m\{\cdot\} \cdot \left(\mathbf{T}_V^{-1} \cdot \mathbf{D}_V^{N_T} \cdot \widehat{\mathbf{T}}_I\right),\end{aligned} \tag{10}$$

where

$$\widehat{\mathbf{H}}^m\{\cdot\} = \left[\begin{array}{c|c} \operatorname{diag}\left\{\widehat{H}_i^m\{\cdot\}\right\} & \mathbf{0}_{(\min\{n_R,n_T\})\times(n-\min\{n_R,n_T\})} \\ \hline \mathbf{0}_{(n-\min\{n_R,n_T\})\times(\min\{n_R,n_T\})} & \mathbf{0}_{(n-\min\{n_R,n_T\})\times(n-\min\{n_R,n_T\})} \end{array}\right], \quad i = 1, \ldots, \min\{n_R, n_T\}, \tag{11}$$

is an $n \times n$ matrix operator whose nonzero elements $\widehat{H}_i^m\{\cdot\}$, $i = 1, \ldots, \min\{n_R, n_T\}$, are (i) the singular values of $\mathbf{H}^+\{\cdot\}$ and (ii) the end-to-end SVD modal transfer functions. $[\cdot]^H$ denotes the Hermitian conjugate of a matrix, $\mathbf{0}_{m\times n}$ is an $m \times n$ matrix with zero elements, and $\widehat{\mathbf{T}}_V$ and $\widehat{\mathbf{T}}_I$ are $n \times n$ unitary matrices [39, 40, 49, 52]. From (10) and (11), the SVD modal transfer function matrix $\widehat{\mathbf{H}}^m\{\cdot\}$ suitable for the MIMO capacity computations of general $n_T \times n_R$ MIMO/BPL systems is determined.

4. Performance and Capacity Metrics of Overhead and Underground MIMO/LV/BPL and MIMO/MV/BPL Systems

In this section, several useful transmission and capacity metrics, which are well proven and used in the communications literature [3, 5, 12–14], are synopsized in order to investigate the behavior of MIMO/BPL channels and systems when UVD modal analysis is applied.

More particularly, the ACG, the RMS-DS, the CB, and various capacity measures—such as cumulative capacity, capacity CCDF, and GC—are reported and applied with the purpose of investigating the transmission and capacity properties of overhead and underground MIMO/LV/BPL and MIMO/MV/BPL channels and systems. All these performances and capacity metrics are based on (i) extended channel transfer functions elements $H_{ij}^+\{\cdot\}$, $i, j = 1, \ldots, n$ of MIMO/BPL transmission channels—as given by (9), and (ii) end-to-end SVD modal transfer function elements $\widehat{H}_i\{\cdot\}$, $i = 1, \ldots, \min\{n_R, n_T\}$—as given by (10)—of MIMO/BPL transmission channels.

4.1. The Discrete Impulse Response. Once the extended channel transfer functions $H_{ij}^+\{\cdot\}$, $i, j = 1, \ldots, n$, of MIMO channels are known from (9), discrete extended impulse responses $h_{ij,p}^+ = h_{ij}^+(t = pT_s)$, $p = 0, \ldots, J-1$, $i, j = 1, \ldots, n$, are obtained as the power of two J-point inverse discrete Fourier transform (IDFT) of the discrete extended channel transfer functions of MIMO channels:

$$\begin{aligned}H_{ij,q}^+ &= \left\{\begin{matrix}\left|H_{ij,q}^+\right| e^{j\varphi_q^+}, & q = 0, \ldots, K-1 \\ 0, & q = K, \ldots, J-1\end{matrix}\right\} \\ &= \left\{\begin{matrix}H_{ij}^+(f = qf_s), & q = 0, \ldots, K-1 \\ 0, & q = K, \ldots, J-1\end{matrix}\right\}, \quad i, j = 1, \ldots, n,\end{aligned} \tag{12}$$

where $F_s = 1/T_s$ is the Nyquist sampling rate, $K \leq J/2$ is the number of subchannels in the BPL signal frequency range of interest, $f_s = F_s/J$ is the flat-fading subchannel frequency spacing, and $|H_{ij,q}^+|$, $i, j = 1, \ldots, n$, and $\phi_{ij,q}^+$, $i, j = 1, \ldots, n$ are the amplitude responses and the phase responses of the discrete extended channel transfer functions of MIMO channels, respectively [71–73].

4.2. The ACG. Since the BPL channels are frequency selective, the ACGs of MIMO channels $\overline{|H_{ij}^+|^2}$, $i, j = 1, \ldots, n$, can be calculated by averaging over frequency [71–73, 76–79]:

$$\overline{\left|H_{ij}^+\right|^2} = \sum_{p=0}^{J-1} \left|h_{ij,p}^+\right|^2 = \frac{1}{J} \sum_{q=0}^{J-1} \left|H_{ij,q}^+\right|^2, \quad i, j = 1, \ldots, n. \tag{13}$$

4.3. The RMS-DS. It is a measure of the multipath richness of a BPL channel. The RMS-DS of MIMO channels $\sigma_{ij,\tau}^+$, $i, j = 1, \ldots, n$, is determined from the following, [71–73, 76–79]:

$$\sigma_{ij,\tau}^+ = T_s \sqrt{\mu_{ij,0}^{(2)} - \left(\mu_{ij,0}\right)^2}, \quad i, j = 1, \ldots, n, \tag{14}$$

where

$$\mu_{ij,0} = \frac{\sum_{p=0}^{J-1} p\left|h_{ij,p}^{+}\right|^2}{\sum_{p=0}^{J-1}\left|h_{ij,p}^{+}\right|^2}, \quad i,j = 1,\ldots,n, \tag{15a}$$

$$\mu_{ij,0}^{(2)} = \frac{\sum_{p=0}^{J-1} p^2\left|h_{ij,p}^{+}\right|^2}{\sum_{p=0}^{J-1}\left|h_{ij,p}^{+}\right|^2}, \quad i,j = 1,\ldots,n. \tag{15b}$$

4.4. The CB. It is the range of frequencies over which the normalized autocorrelation function of the channel transfer function is over a certain CB correlation level X (usually set to 0.9, 0.7, or 0.5), that is, the maximum bandwidth in which the subchannels can be approximately considered flat-fading. As the phase response of the extended channel transfer function may be assumed as uniformly distributed over $[0, 2\pi]$, the CB of MIMO channels can be determined from the following [47, 80–82, 109]:

$$B_{ij,c}(\Delta f) = \frac{E\left\{H_{ij,q}^{+}\cdot\left[H_{ij}^{+}(f = qf_s + \Delta f)\right]^*\right\}}{E\left\{\left|H_{ij,q}^{+}\right|^2\right\}},$$
$$q = 0,1,\ldots,\left\lfloor (J-2) + \frac{\Delta f}{f_s}\right\rfloor, \quad i,j = 1,\ldots,n, \tag{16}$$

where Δf is the frequency shift, $[\cdot]^*$ denotes the complex conjugate of an element, and $\lfloor x\rfloor$ is the largest integer not greater than x. From (16), $\mathrm{CB}_{ij,X}$, $i, j = 1,\ldots,n$, is that value of Δf such that $B_{ij,c}(\Delta f) = X$, $i, j = 1,\ldots,n$.

4.5. The Capacity. Capacity is the maximum achievable transmission rate over a BPL channel. Note that, in the rest of this review paper, the common case is examined where the transmitting end does not have channel state information (CSI) [13, 14]. In the general case of $n_T \times n_R$ MIMO/BPL systems, the MIMO capacity is calculated by using the following [13, 14, 33, 41, 42, 48, 50, 53–55]:

$$C^{\mathrm{MIMO}} = f_s \sum_{q=0}^{J-1}\sum_{i=1}^{\min\{n_T,n_R\}} \log_2\left\{1 + \frac{\mathrm{SNR}(qf_s)}{n_T}\cdot\left|\widehat{H}_i^{m}(qf_s)\right|^2\right\}, \tag{17}$$

where

$$\mathrm{SNR}(f) = \frac{p(f)}{N(f)} \tag{18}$$

is the BPL signal-to-noise ratio (SNR), $p(f)$ is the selected injected power spectral density mask (IPSDM)—that is recommended by the regulation authorities—and $N(f)$ is the channel noise PSD [16, 37, 110].

As less transmit and receive ports are deployed, the capacity results tend to present the capacity results of SISO/BPL systems. More specifically, depending on the number of transmit and receive ports, appropriate well-known capacity expressions can be used—see also [13, 14, 41, 42].

(i) *Single-Input Multiple-Output (SIMO) Capacity Expression*. When one transmit and n_R, $1 < n_R \leq n$, receive ports occur.

(ii) *Multiple-Input Single-Output (MISO) Capacity Expression*. When n_T, $1 < n_T \leq n$, transmit and one receive ports occur.

(iii) *SISO Capacity Expression*. When one transmit and one receive ports occur.

According to the aforementioned different MIMO, SIMO, MISO, and SISO scheme configurations, the resulting single- and multiport diversities may be classified into two major classes [13, 14].

(i) *Pure Scheme Configurations*. This class contains the elementary single- and multiport implementations, namely, $n \times n$ MIMO, $1 \times n$ SIMO, $n \times 1$ MISO, and all SISO systems.

(ii) *Mixed Scheme Configurations*. This class contains all the other multiport implementations that may be deployed.

On the basis of the previous capacity expressions, three additional capacity measures are reported and are applied in the following analysis.

(i) *Cumulative Capacity*. The cumulative capacity is the cumulative upper limit of information which can be reliably transmitted over the end-to-end BPL channel. In fact, cumulative capacity describes the aggregate capacity effect of all subchannels of the examined frequency band [13, 14].

(ii) *Capacity CCDF*. The capacity CCDF defines the statistics of cumulative capacity of BPL channels, specifying the cumulative capacity probability of exceeding a specific cumulative capacity threshold [13, 14].

(iii) *GC*. The GC is introduced as the ratio of the MIMO cumulative capacity of a BPL system over its respective SISO one (usually set to SISO/CC which is the best today's BPL system cumulative capacity).

5. Numerical Results and Discussion

The simulations of various types of overhead and underground MIMO/LV/BPL and MIMO/MV/BPL transmission channels and systems aim at investigating (a) their broadband MIMO transmission characteristics; (b) how their spectral behavior is affected by several factors; (c) statistical remarks obtained on the basis of simulated overhead and underground LV/BPL and MV/BPL MTL configurations; and (d) how the capacity measures are influenced by the implementation of various MIMO/BPL scheme configurations.

For the numerical computations, the overhead and underground LV and MV distribution line configurations depicted in Figures 1(a)–1(d) have been considered. As mentioned in Section 3.1, since the modes supported by the overhead and underground LV/BPL and MV/BPL configurations may be examined separately, it is assumed for simplicity

that the BPL signal is injected directly into the EVD modes [15–18, 57–65, 67]; thus, the complicated EVD and SVD modal analyses of [13, 14, 41, 42, 60, 61, 81], briefly outlined in Section 3.2, are bypassed, and the practical implementation of UVD modal analysis is further facilitated.

As it concerns the simulation model properties, the Nyquist sampling rate F_s and flat-fading subchannel frequency spacing f_s are assumed equal to 200 MHz and 0.1 MHz, respectively. Moreover, the number of subchannels K in the BPL signal frequency range of interest and the J-point IDFT are assumed equal to 991 and 2048, respectively [71–73, 111, 112].

As it regards the overhead and underground LV/BPL and MV/BPL MTL configurations, the simple BPL topology of Figure 2 having N branches is considered. Based on [15–18, 57, 58, 67, 87] and with reference to Figure 2, the transmitting and the receiving ends are assumed matched to the characteristic impedance of the mode considered, whereas the branch terminations Z_{bk}, $k = 1, \ldots, N$, connected at positions A'_k, $k = 1, \ldots, N$, respectively, are assumed open circuits. Path lengths $\sum_{k=1}^{N+1} L_k$ of the order of 200 m are encountered in underground BPL transmission [83, 87, 92]. These path lengths are quite shorter compared to the overhead BPL case where path lengths up to 1000 m may be encountered [16, 18, 20, 21, 57, 58, 62, 67, 83, 85, 87, 92, 99, 113, 114].

With reference to Figure 2, five indicative overhead topologies, which are common for both overhead LV/BPL and MV/BPL systems, concerning end-to-end connections of average lengths equal to 1000 m have been examined [13, 14, 16].

(1) A typical overhead urban topology (overhead urban case A) with $N = 3$ branches ($L_1 = 500$ m, $L_2 = 200$ m, $L_3 = 100$ m, $L_4 = 200$ m, $L_{b1} = 8$ m, $L_{b2} = 13$ m, and $L_{b3} = 10$ m).

(2) An aggravated overhead urban topology (overhead urban case B) with $N = 5$ branches ($L_1 = 200$ m, $L_2 = 50$ m, $L_3 = 100$ m, $L_4 = 200$ m, $L_5 = 300$ m, $L_6 = 150$ m, $L_{b1} = 12$ m, $L_{b2} = 5$ m, $L_{b3} = 28$ m, $L_{b4} = 41$ m, and $L_{b5} = 17$ m).

(3) A typical overhead suburban topology (overhead suburban case) with $N = 2$ branches ($L_1 = 500$ m, $L_2 = 400$ m, $L_3 = 100$ m, $L_{b1} = 50$ m, and $L_{b2} = 10$ m).

(4) A typical overhead rural topology (overhead rural case) with only $N = 1$ branch ($L_1 = 600$ m, $L_2 = 400$ m, and $L_{b1} = 300$ m).

(5) The overhead "LOS" transmission along the same end-to-end distance $L = L_1 + \cdots + L_{N+1} = 1000$ m when no branches are encountered. It corresponds to the line-of-sight (LOS) path in wireless transmission.

The respective indicative underground BPL topologies, which are common for both underground LV/BPL and MV/BPL systems, concern 200 m long end-to-end connections. These topologies are [13, 14, 16, 18] as follows.

(1) A typical underground urban topology (underground urban case A) with $N = 3$ branches ($L_1 = 70$ m, $L_2 = 55$ m, $L_3 = 45$ m, $L_4 = 30$ m, $L_{b1} = 12$ m, $L_{b2} = 7$ m, and $L_{b3} = 21$ m).

(2) An aggravated underground urban topology (underground urban case B) with $N = 5$ branches ($L_1 = 40$ m, $L_2 = 10$ m, $L_3 = 20$ m, $L_4 = 40$ m, $L_5 = 60$ m, $L_6 = 30$ m, $L_{b1} = 22$ m, $L_{b2} = 12$ m, $L_{b3} = 8$ m, $L_{b4} = 2$ m, and $L_{b5} = 17$ m).

(3) A typical underground suburban topology (underground suburban case) with $N = 2$ branches ($L_1 = 50$ m, $L_2 = 100$ m, $L_3 = 50$ m, $L_{b1} = 60$ m, and $L_{b2} = 30$ m).

(4) A typical underground rural topology (rural case) with only $N = 1$ branch ($L_1 = 50$ m, $L_2 = 150$ m, and $L_{b1} = 100$ m).

(5) The underground "LOS" transmission along the same end-to-end distance $L = L_1 + \cdots + L_{N+1} = 200$ m when no branches are encountered.

Finally, as it concerns the properties of MIMO/BPL scheme configurations, the proposed study of general $n_T \times n_R$ MIMO/BPL systems—outlined in Sections 3.1 and 3.2—via UVD modal analysis is considered. To evaluate the capacity performance of overhead and underground MIMO/LV/BPL and MIMO/MV/BPL transmission channels and systems, in the case of overhead BPL transmission, a uniform additive white Gaussian noise (AWGN) PSD level is assumed equal to −105 dBm/Hz [16, 18, 57, 67] that is higher compared to the significantly lower AWGN/PSD encountered in underground BPL transmission assumed equal to −135 dBm/Hz [18, 97, 115–117]. As it is usually done [13, 14], the noise AWGN/PSD of each power grid type is assumed common (i) between corresponding LV and MV systems and (ii) among all MIMO channels of the same MTL configuration. With regard to power constraints in the 3–88 MHz frequency range, the same IPSDM limits between LV/BPL and MV/BPL are assumed [13, 14, 16, 18, 118, 119]. In detail, at frequencies below 30 MHz, according to Ofcom, in the 1.705–30 MHz frequency range maximum levels of −60 dBm/Hz and −40 dBm/Hz constitute appropriate IPSDMs for overhead and underground MIMO/BPL systems, respectively, providing presumption of compliance with the current FCC Part 15 limits [16, 18, 118, 119]. In the 30–88 MHz frequency range, maximum IPSDM levels equal to −77 dBm/Hz and −57 dBm/Hz for overhead and underground MIMO/BPL systems, respectively, are assumed to provide a presumption of compliance in this frequency range [16, 18, 118, 119].

5.1. Channel Attenuation of Overhead and Underground MIMO/LV/BPL and MIMO/MV/BPL Channels: Comparison of UVD Modal Analysis—Results with Other Already Validated Ones. In Figures 3(a) and 3(b), the median values of channel attenuation in the frequency band 1–100 MHz for CCs (solid lines) and for XCs (dashed lines) are plotted with respect to frequency for the aforementioned indicative overhead LV/BPL and MV/BPL topologies, respectively, in the frequency range 1–100 MHz. In Figures 3(c) and 3(d), the same curves are plotted in the case of underground LV/BPL and MV/BPL systems, respectively.

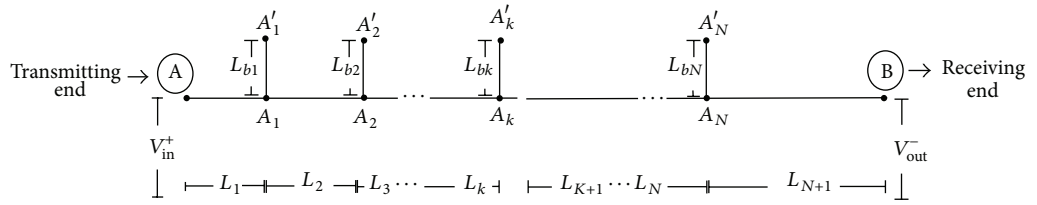

FIGURE 2: End-to-end BPL connection with N branches [16, 18].

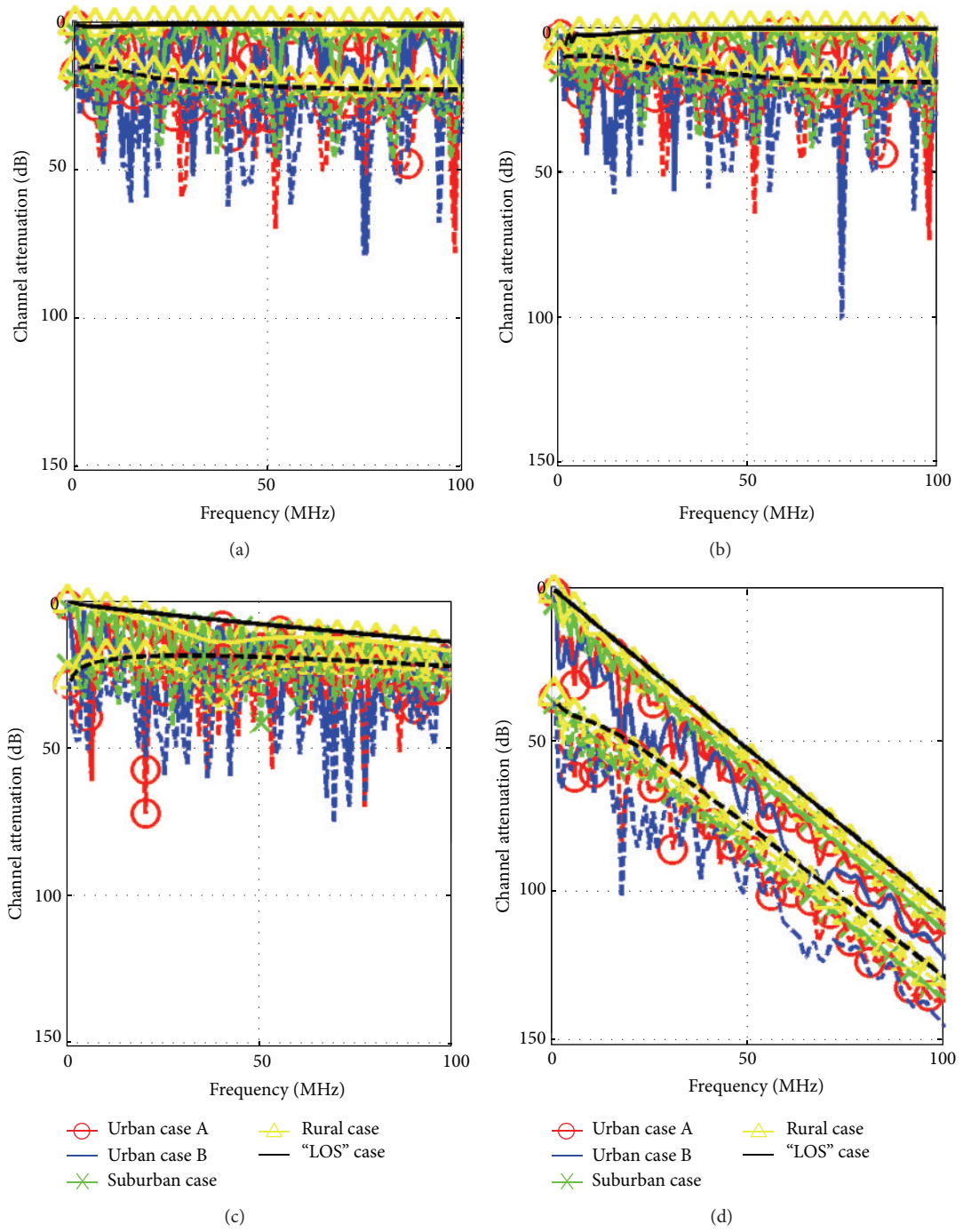

FIGURE 3: Frequency spectra of attenuation coefficients of MIMO/BPL channels: CCs (solid lines) and XCs (dashed lines)—the subchannel frequency spacing is equal to 1 MHz. (a) Overhead LV. (b) Overhead MV. (c) Underground LV. (d) Underground MV.

Table 1: Statistical values of ACG for various overhead and underground MIMO/LV/BPL and MIMO/MV/BPL channels.

	ACG (dB)							
	Min		Max		Mean		Standard deviation	
	OV	UN	OV	UN	OV	UN	OV	UN
CC								
LV	−12.70	−19.18	−4.63	−9.46	**−8.36**	**−14.13**	**3.03**	**3.63**
MV	−13.01	−27.64	−4.92	−18.44	**−8.67**	**−23.40**	**3.04**	**3.62**
XC								
LV	−29.54	−31.30	−23.17	−23.23	**−26.04**	**−26.94**	**2.67**	**3.05**
MV	−24.64	−61.19	−17.99	−54.14	**−20.99**	**−57.71**	**2.74**	**2.83**
All								
LV	−29.54	−31.30	−4.63	−9.46	−17.20	−20.54	9.70	7.45
MV	−24.64	−61.19	−4.92	−18.44	−14.83	−40.55	7.04	18.34

OV: overhead, UN: underground.

Observations based on Figures 3(a)–3(d) were made as follows.

(i) Comparing Figures 3(a) and 3(c) with the respective Figures 3(a) and 3(b) of [14], it is evident that UVD modal analysis combined with TM1 method gives almost identical channel attenuation results with the corresponding ones of SVD modal analysis when it is combined with the accurate TM2 method for overhead and underground MIMO/LV/BPL channels, respectively. The same high channel attenuation precision is also achieved when Figures 3(b) and 3(d) are compared with the respective Figures 3(a) and 3(c) of [13]. Again, UVD modal analysis combined with TM1 method gives the same attenuation results with those derived from the combination of SVD modal analysis with TM1 method for overhead and underground MIMO/MV/BPL channels, respectively. Therefore, UVD modal analysis offers excellent accuracy for all overhead and underground MIMO/LV and MIMO/MV BPL channels that are examined across this review paper.

(ii) Due to the common bus-bar system topology [13, 14, 54, 78], in overhead and underground LV/BPL and MV/BPL systems, the channel attenuation curves between CCs and XCs present similarities concerning their curve slopes and the position and extent of spectral notches. This indicates the strong coupling between the individual MIMO channels. Actually, the attenuation of MIMO channels depends drastically on the frequency, the power grid type, the MIMO channel type, the MTL configuration, the physical properties of the cables used, the end-to-end—"LOS"—distance, and the number, the electrical length, and the terminations of the branches encountered along the end-to-end BPL signal transmission path [15, 16, 18, 24, 66, 92, 99, 113, 120].

(iii) Regardless of the power grid type and power grid topology, XCs present higher channel attenuations in comparison with CCs ones [48, 53, 55]. The channel attenuation difference between CCs and XCs for the same topology exceeds 15 dB in most of the cases [13, 14].

(iv) In accordance with [15–18, 37] and based on the picture of the spectral behavior observed from Figures 3(a)–3(d), the overhead and underground MIMO/LV/BPL and MIMO/MV/BPL channels may be classified into three channel classes: "LOS," good, and bad channels.

(v) Due to the favorable low-loss transmission characteristics of overhead MIMO/LV/BPL, overhead MIMO/MV/BPL, and underground MIMO/LV/BPL channels, these power grid types can define an excellent cooperative communications platform that is suitable for last mile broadband communications services [15–18, 83, 87, 91, 92, 94, 121].

5.2. ACG. Hereafter, it is assumed for simplicity that only the median values of ACG over CCs and XCs for each of the aforementioned indicative overhead and underground LV/BPL and MV/BPL topologies will be studied in the frequency band 1–100 MHz.

In Table 1, the minimum value, the maximum value, the mean, and the standard deviation of the ACG for the overhead and underground MIMO/LV/BPL and MIMO/MV/BPL channels (CC, XC, and all together) are reported.

In Figure 4(a), the quantile-quantile plots of the ACG of MIMO channels for the indicative overhead LV/BPL and MV/BPL topologies are depicted in order to examine the normality of the ACG distribution functions [78]. In these plots, the sample quantiles of ACGs are displayed versus theoretical quantiles from normal distributions. In Figure 4(b), the ACG CDF curves of MIMO channels (dashed lines) for the same overhead LV/BPL and MV/BPL topologies are also plotted. Four CDF curves of four random variables normally distributed with mean and standard deviation reported in Table 1 (overhead LV/CC, overhead LV/XC, overhead MV/CC, and overhead MV/XC) are also drawn (bold lines). Finally, a unified ACG CDF curve, which is normally distributed and is

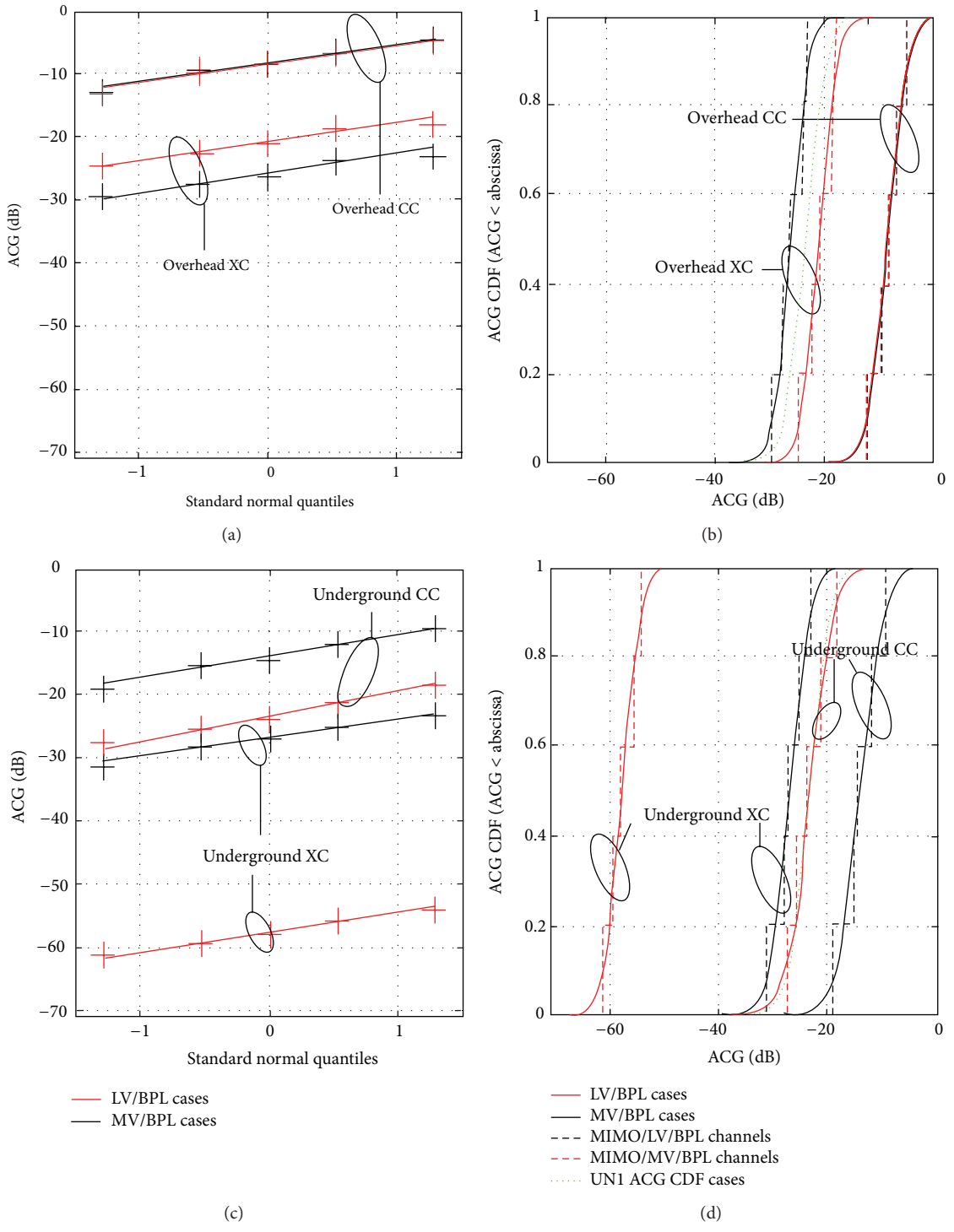

Figure 4: (a) Quantile-quantile ACG plots of overhead MIMO/LV/BPL (+) and MIMO/MV/BPL (+) channels compared to theoretical normal distribution lines of overhead LV/BPL and MV/BPL cases. (b) ACG CDF curves of overhead MIMO/LV/BPL and MIMO/MV/BPL channels compared to theoretical normal distribution lines of overhead LV/BPL, overhead MV/BPL, and UN1 ACG CDF cases. (c), (d) Similar plots in underground BPL cases.

common for all overhead and underground MIMO/LV/BPL and MIMO/MV/BPL channels—detailed in the following analysis—is also given. In Figures 4(c) and 4(d), similar plots are displayed in the case of underground LV/BPL and MV/BPL MIMO channels.

From Figures 4(a)–4(d), the following are clearly demonstrated.

(i) Despite the power grid type, ACG curves of MIMO channels follow normal distributions. This is

explained observing the simulation plots that are close to linear ones (bold lines). The lognormality (normality) of the ACG may be justified by the multipath nature of BPL signal propagation and the TL modeling based on cascaded two-port network modules [4, 71–73].

(ii) The ACG curves can be fitted by appropriate lognormal distributions for each overhead and underground LV/BPL and MV/BPL topology. Small deviations may occur for BPL topologies with small electrical length. Recently, suitable lognormal distributions have been proposed in the analysis of various SISO/BPL channels [4, 31, 56, 71–73, 78, 79].

(iii) As expected, the spectral behavior of overhead and underground MIMO/LV/BPL and MIMO/MV/BPL channels depicted in Figures 3(a)–3(d) is reflected on respective ACG distributions. Indeed, the ACG distributions of underground MV/BPL transmission are significantly worse than those of other power grid types.

(iv) Examining ACG metric, it is verified that CCs demonstrate better transmission characteristics in comparison with XCs regardless of the power grid type and power grid topology. Due to these favorable characteristics of CCs, their exploitation is mainly promoted during the implementation of SISO/BPL systems. Actually, this is the typical SISO/BPL implementation scheme in today's BPL networks.

(v) From Table 1 and Figures 4(b) and 4(d), in order to promote the common ACG CDF curve analysis of overhead and underground MIMO/LV/BPL and MIMO/MV/BPL channels, a unified ACG CDF curve is considered. This ACG CDF curve, which is denoted as UN1 ACG CDF, is normally distributed with mean (mean of the eight abovementioned ACG CDF means) and standard deviation (mean of the eight abovementioned ACG CDF standard deviations) equal to 23.28 μs and 3.08 μs, respectively. The UN1 ACG CDF curve allows the introduction of common ACG CDF curve analysis regardless of the overhead and underground LV/BPL and MV/BPL topologies delivering a first statistical analysis intuition towards the existing deterministic analysis [71].

5.3. RMS-DS. In this subsection, it is assumed that only the median values of RMS-DS over CCs and XCs for each of the aforementioned indicative overhead and underground LV/BPL topologies will be studied in the frequency band 1–100 MHz.

In Table 2, the minimum value, the maximum value, the mean, and the standard deviation of the RMS-DS for the overhead and underground MIMO/LV/BPL and MIMO/MV/BPL channels (CC, XC, and all together) are reported.

In Figure 5(a), the quantile-quantile plots of the RMS-DS of MIMO channels for the overhead LV/BPL and MV/BPL topologies are depicted in order to test the normality of the RMS-DS distribution functions [78]. In these plots, the sample quantiles of RMS-DS are displayed versus theoretical quantiles from normal distributions. In Figure 5(b), the RMS-DS CDF curves of MIMO channels (dashed lines) for the overhead LV/BPL and MV/BPL topologies are plotted. Four CDF curves of four random variables that are normally distributed with mean and standard deviation reported in Table 2 (overhead LV/CC, overhead LV/XC, overhead MV/CC, and overhead MV/XC) are also plotted (bold lines). Finally, a unified RMS-DS CDF curve that is normally distributed, which is common for both overhead and underground MIMO/LV/BPL and MIMO/MV/BPL channels and is detailed in the following analysis, is also given. In Figures 5(c) and 5(d), similar plots are given in the case of underground MIMO/LV/BPL and MIMO/MV/BPL channels.

From Figures 5(a)–5(d), the following are observed.

(i) RMS-DS is lognormally distributed with good approximation in all overhead and underground MIMO/LV/BPL and MIMO/MV/BPL channels for all overhead and underground LV/BPL and MV/BPL topologies [4, 31, 56, 71–73, 78, 79]. However, RMS-DS is highly variable depending on power grid type and power grid topology while RMS-DS increases as the topology complexity rises. In fact, bad channel class presents higher RMS-DS values than those of "LOS" and good channel classes due to the existing aggravated multipath environment [47, 122].

(ii) In general, overhead MIMO/LV/BPL, overhead MIMO/MV/BPL, and underground MIMO/MV/BPL channels present comparable RMS-DS results. However, underground MIMO/LV/BPL channels present lower RMS-DS values than those of the aforementioned three MIMO/BPL systems. This renders underground MIMO/LV/BPL transmission as more multipath resistant and more appropriate for sensitive SG applications.

(iii) From Table 2 and Figures 5(b) and 5(d), in order to bypass the RMS-DS CDF dependency on power grid type and power grid topologies, a unified RMS-DS CDF—denoted as UN1 RMS-DS CDF—normally distributed with mean (mean of the eight aforementioned RMS-DS CDF means) and standard deviation (mean of the eight aforementioned RMS-DS CDF standard deviations) equal to 0.83 μs and 0.40 μs, respectively, is considered. The UN1 RMS-DS CDF curve allows the replication of the variability of overhead and underground LV/BPL and MV/BPL topologies conferring a stochastic aspect to the existing deterministic analysis [71].

Analyzing the statistical performance metrics of Tables 1 and 2, a fundamental property of several wireline channels (e.g., DSL, coaxial, and phone links) may be also pointed out in the overhead and underground MIMO/LV/BPL and MIMO/MV/BPL channels: the correlation between ACG and RMS-DS. This correlation can be easily confirmed simply by observing the scatter plot presented in Figures 6(a) and 6(b) where the above set of numerical results of MIMO channels

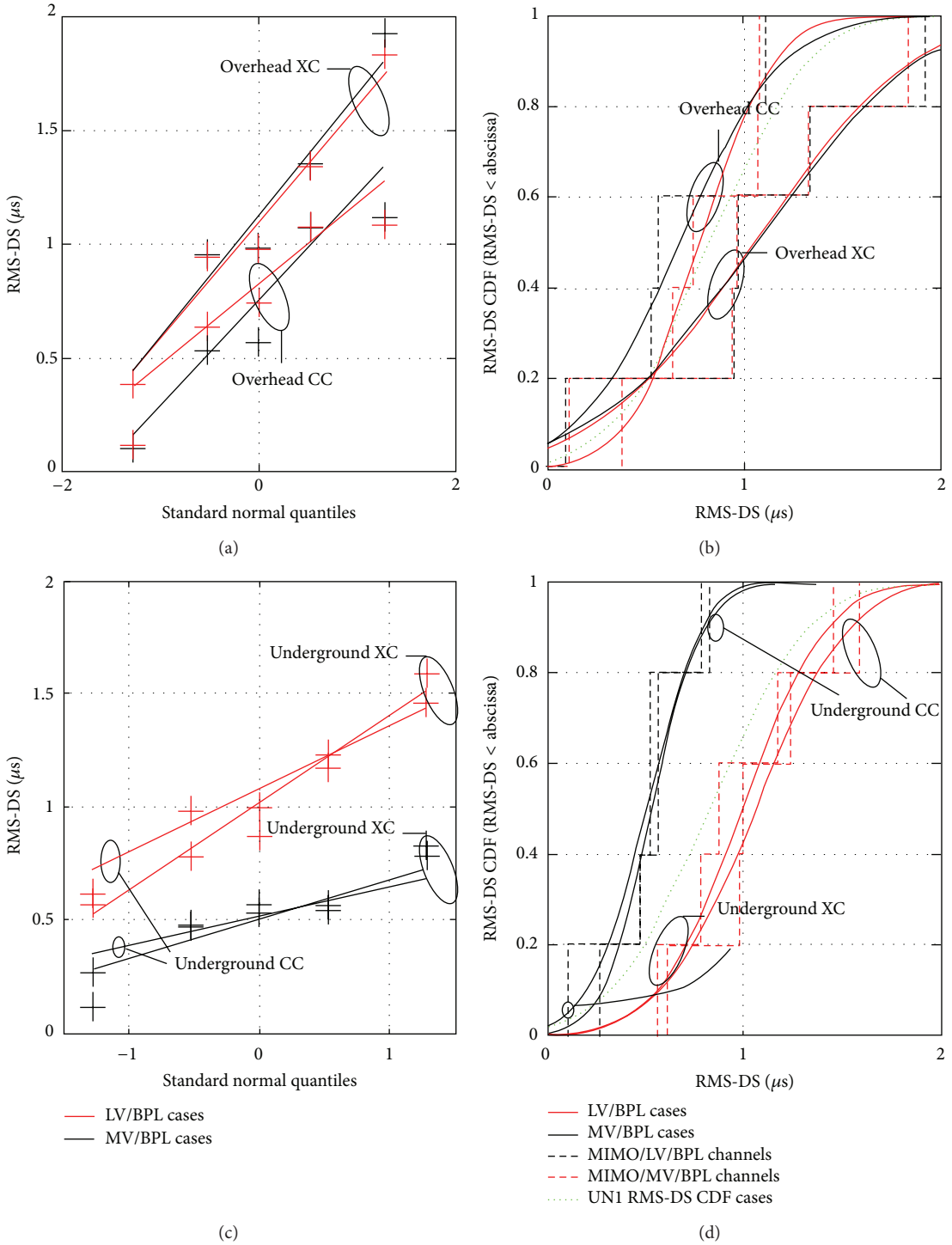

FIGURE 5: (a) Quantile-quantile plots of RMS-DS of overhead MIMO/LV/BPL (+) and MIMO/MV/BPL (+) channels compared to theoretical normal distribution lines of overhead LV/BPL and MV/BPL cases. (b) RMS-DS CDFs of overhead MIMO/LV/BPL and MIMO/MV/BPL channels compared to theoretical normal distribution lines of overhead LV/BPL, overhead MV/BPL, and UN1 RMS-DS CDF cases. (c), (d) Similar plots in underground BPL cases.

Table 2: Statistical values of RMS-DS for various overhead and underground MIMO/LV/BPL and MIMO/MV/BPL channels.

	RMS-DS (μs)							
	Min		Max		Mean		Standard deviation	
	OV	UN	OV	UN	OV	UN	OV	UN
CC								
LV	0.09	0.26	1.12	0.83	**0.68**	**0.53**	**0.42**	**0.20**
MV	0.38	0.61	1.08	1.46	**0.78**	**1.00**	**0.30**	**0.34**
XC								
LV	0.11	0.11	1.92	0.78	**1.06**	**0.50**	**0.66**	**0.24**
MV	0.11	0.56	1.84	1.59	**1.04**	**1.06**	**0.63**	**0.37**
All								
LV	0.11	0.11	1.92	0.78	1.06	0.50	0.66	0.25
MV	0.28	0.56	1.81	1.59	1.11	1.06	0.55	0.37

OV: overhead, UN: underground.

for the aforementioned indicative overhead and underground BPL topologies, respectively, are plotted.

In Figures 6(a) and 6(b), except for the numerical results, a set of regression trend lines is also presented, namely,

(i) regression line set of the form $(\sigma_\tau)_{\mu s} = -\nu \cdot (\overline{|H|^2})_{\text{dB}} + w$, where $(\overline{|H|^2})_{\text{dB}}$ is the ACG in dB and $(\sigma_\tau)_{\mu s}$ is the RMS-DS in μs of the MIMO/LV/BPL and MIMO/MV/BPL channels, which are examined. Analytically, the regression trend lines are as follows:

(1) ANT approach, as given by [78], with robust regression parameters ν and w assumed equal to 0.0197 μs/dB and 0 μs, respectively;

(2) GAL approach, as given by [71–73], with robust regression parameters assumed ν = 0.0075 μs/dB and w = 0.183 μs;

(3) the proposed UN1$^{\text{OV}}$, UN1$^{\text{UN}}$, and UN1 approaches with regression parameters $[\nu, w]$ equal to $[-0.0303\,\mu\text{s/dB}, 0.4066\,\mu\text{s}]$, $[-0.01265\,\mu\text{s/dB}, 0.3829\,\mu\text{s}]$, and $[-0.01029\,\mu\text{s/dB}, 0.591\,\mu\text{s}]$, respectively. The least squares fitting method is applied to the aforementioned overhead, underground, and all together numerical results for the evaluation of parameters $[\nu, w]$ of UN1$^{\text{OV}}$, UN1$^{\text{UN}}$, and UN1 approaches, respectively.

From Figures 6(a) and 6(b), the following should be mentioned.

(i) In spite of the power grid type, power grid topology, and MIMO/BPL channel type, the negative slopes of all regression lines clearly confirm that the ACG and RMS-DS of overhead and underground MIMO/LV/BPL and MIMO/MV/BPL channels are negatively correlated lognormal random variables.

(ii) The existing regression trend lines (ANT and GAL approaches) in the literature [71–73, 78] better describe the correlation between RMS-DS and ACG in underground BPL systems rather than in overhead ones. This is due to the fact that the 1000 m long overhead connections present high-multipath behavior compared to the 200 m long connections of the underground case where "LOS" attenuation is the primary attenuation mechanism.

(iii) On the basis of the correlation between ACG and RMS-DS, three new approximations are proposed, which are suitable for the BPL statistical channel modeling where this correlation is imposed by design [71–73]. The proposed UN1$^{\text{OV}}$, UN1$^{\text{UN}}$, and UN1 regression lines suggest a unified regression approach that describes the ACG and RMS-DS correlation between overhead, underground, and all together MIMO channels, respectively, regardless of the power grid type level (either LV or MV), power grid topology, and MIMO/BPL channel type.

5.4. CB. In the rest of this subsection, it is assumed that only the median values of CB over CCs and XCs for each of the aforementioned indicative overhead and underground LV/BPL and MV/BPL topologies will be studied in the frequency band 1–100 MHz.

In Table 3, the minimum value, the maximum value, the mean, and the standard deviation of the $\text{CB}_{0.5}$ for the overhead and underground MIMO/LV/BPL and MIMO/MV/BPL channels (CC, XC, and all together) are presented.

Observing statistical performance metrics of Tables 2 and 3, a second fundamental property of several wireline systems is also validated in the overhead and underground MIMO/LV/BPL and MIMO/MV/BPL channel cases: the correlation between CB and RMS-DS. In Figures 7(a) and 7(b), the scatter plots of the RMS-DS versus the $\text{CB}_{0.5}$ for the numerical results of overhead and underground channels, respectively, are presented. Apart from the numerical results, a set of proposed regression trend lines is also given:

(i) hyperbolic trend lines set of the form $(\sigma_\tau)_{\mu s} = y \cdot (\text{CB}_{0.5})_{\text{MHz}}$, where $(\text{CB}_{0.5})_{\text{MHz}}$ is the $\text{CB}_{0.5}$ in MHz: (i) the proposed UN2$^{\text{OV}}$, UN2$^{\text{UN}}$, and UN2

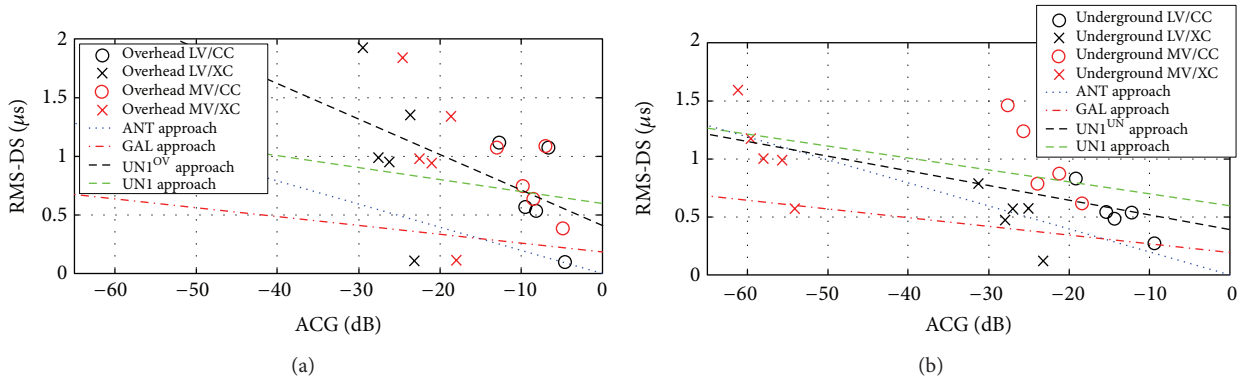

(a) (b)

Figure 6: Scatter plot of RMS-DS versus ACG for simulated MIMO/LV/BPL and MIMO/MV/BPL channels and various regression approaches. (a) Overhead. (b) Underground.

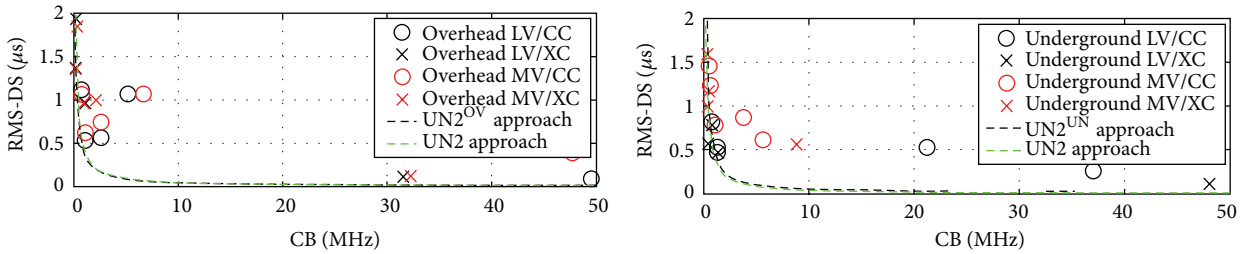

(a) (b)

Figure 7: Scatter plot of RMS-DS versus $CB_{0.5}$ for simulated MIMO/LV/BPL and MIMO/MV/BPL channels and various regression approaches. (a) Overhead. (b) Underground.

approaches with parameter y assumed equal to 0.3921 μs·MHz, 0.4555 μs·MHz, and 0.4155 μs·MHz, respectively, obtained using robust linear least square error fitting between the trend line and the observed overhead, underground, and all together numerical results, respectively.

On the basis of the second fundamental property, which is confirmed for overhead and underground MIMO/LV/BPL and MIMO/MV/BPL channels, additional observations are added [100, 123–125].

(i) CB and RMS-DS are inversely related and their relation can be approximated by appropriate hyperbolic functions. $UN2^{OV}$, $UN2^{UN}$, and UN2 approaches are in very good agreement with the overhead, underground, and all together simulation results, respectively, proposing a unified consideration of the CB/RMS-DS correlation.

(ii) The variability of the pair values of $CB_{0.5}$ and RMS-DS primarily depends on the power grid type, the overhead and underground MIMO/LV/BPL and MIMO/MV/BPL channel types, and the power grid topology characteristics.

(iii) $UN2^{OV}$, $UN2^{UN}$, and UN2 approaches quantify the effects of frequency selective behavior. Despite the CB and RMS-DS differences between overhead and underground LV/BPL and MV/BPL channels due to multipath environment and "LOS" attenuation, $UN2^{OV}$ and $UN2^{UN}$ approaches accurately fit the numerical results of overhead and underground MIMO/BPL channels, respectively. Taking under consideration the almost identical $UN2^{OV}$ and $UN2^{UN}$ behaviors, UN2 approach promotes an elementary step towards a common transmission handling between overhead and underground LV/BPL and MV/BPL systems. More specifically, UN2 approach fits very well either numerical results or $UN2^{OV}$ and $UN2^{UN}$ approaches regardless of the power grid type, power grid topology, and MIMO channel type.

(iv) Except for $UN1^{OV}$, $UN1^{UN}$, and UN1 regression lines that have been proposed for the wireline statistical channel modeling by design, $UN2^{OV}$, $UN2^{UN}$, and UN2 approaches may operate as evaluation metrics of the applied statistical channel models [71–79].

5.5. Capacity. The potential transmission performance in terms of capacity in the frequency range 3–88 MHz is evaluated under the assumption of Ofcom/IPSDMs and AWGN/PSDs that have been presented in the introduction of Section 4. Moreover, in this subsection, it is assumed that only the median values of SISO capacities over CCs and

Table 3: Statistical values of $CB_{0.5}$ for various overhead and underground MIMO/LV/BPL and MIMO/MV/BPL channels.

	$CB_{0.5}$ (MHz)							
	Min		Max		Mean		Standard deviation	
	OV	UN	OV	UN	OV	UN	OV	UN
CC								
LV	0.70	0.80	49.50	37	11.82	12.32	21.14	16.31
MV	0.80	0.50	47.60	5.60	11.78	2.32	20.16	2.28
XC								
LV	0.20	0.40	31.50	48	7.00	10.20	13.72	21.13
MV	0.20	0.30	32.20	8.80	7.16	2.06	14.02	3.77
All								
LV	0.20	0.40	32.50	48	7.20	10.20	14.16	21.13
MV	0.20	0.30	27	8.80	5.76	2.06	11.88	3.77

OV: overhead, UN: underground.

XCs for each of the aforementioned indicative overhead and underground LV/BPL and MV/BPL topologies will be investigated (see details in [13, 14]).

In Figures 8(a) and 8(b), the respective SISO cumulative capacities of the LV/BPL and MV/BPL systems for the aforementioned indicative overhead topologies are plotted with respect to frequency. In Figure 8(c), the SISO capacity CCDF curves for the overhead LV/BPL and MV/BPL systems are drawn. In Figures 8(d)–8(f), similar plots are given in the case of underground LV/BPL and MV/BPL systems.

From Figures 8(a)–8(f), the following are observed.

(i) As it has already been mentioned, the analysis concerning general $n_T \times n_R$ MIMO/BPL systems is based on UVD modal analysis concerning MIMO channels. Only in the case of SISO/BPL systems, their behavior is defined directly by the corresponding SISO/BPL—either SISO/CC or SISO/XC—channel characterization.

(ii) The extremely strong attenuation exhibited by underground MV/BPL systems is counterbalanced by the significantly higher IPSDM limits imposed on underground MV/BPL transmission, lower AWGN/PSD, and shorter average end-to-end transmission distances. Thus, the transmission efficiency of underground MIMO/MV/BPL systems becomes comparable to that of overhead LV/BPL and MV/BPL systems [13, 14, 16, 18].

(iii) The significantly higher IPSDM limits combined with shorter average end-to-end transmission distances, low channel attenuation, and low noise characteristics make the transmission efficiency of underground SISO/LV/BPL systems incomparable to the rest of BPL systems [16, 18]. In detail, the capacities of underground SISO/LV/BPL systems are multiple of an approximate factor of 3 in comparison with the capacities of the respective overhead SISO/LV/ BPL, overhead SISO/MV/BPL, and underground SISO/MV/BPL systems. This feature renders underground LV/BPL systems as a BPL backbone network enhancing the necessary intraoperability between overhead and underground LV/BPL and MV/BPL networks.

(iv) In both overhead and underground LV/BPL and MV/BPL topologies, CCs are those that statistically convey higher SISO capacities than XCs. For the overhead LV/BPL and MV/BPL topologies, the 80th percentile of the SISO capacity CCDF curves for CCs is equal to 608 Mbps and 596 Mbps, respectively, while the respective CCDF curves for XCs are equal to 206 Mbps and 293 Mbps, respectively. For the underground LV/BPL and MV/BPL topologies, the 80th percentile of the SISO capacity CCDF curves for CCs is equal to 1849 Mbps and 790 Mbps, respectively, while the respective CCDF curves for XCs are equal to 1514 Mbps and 334 Mbps, respectively. Even if CCs and XCs present similarities as they concern the channel attenuation curves due to the common bus-bar system topologies, their significant difference affects critically the achievable SISO capacities. This yields a disadvantage in practical applications where the coupling scheme applied at transmitting end needs to be the same at the receiving end [78, 126].

Continuing MIMO/BPL capacity analysis, different MIMO/BPL scheme configurations, which are diversified by their number of transmit and receive ports, are investigated for both overhead and underground MIMO/LV/BPL and MIMO/MV/BPL systems [41, 42, 48, 53, 55, 127, 128]. As already described in [13, 14], it is assumed that only the median values of all possible SIMO, MISO, and MIMO system capacities for each of the aforementioned indicative overhead and underground LV/BPL and MV/BPL topologies will be studied.

To investigate the capacity potential of various single- and multiport BPL implementations, pure scheme configurations are first studied and compared by means of their cumulative capacity and capacity CCDF curves. In Figures 9(a), 9(c), and 9(e), the 1×4 SIMO cumulative capacity, the 4×1 MISO capacity, and the 4×4 MIMO capacity, respectively, for the

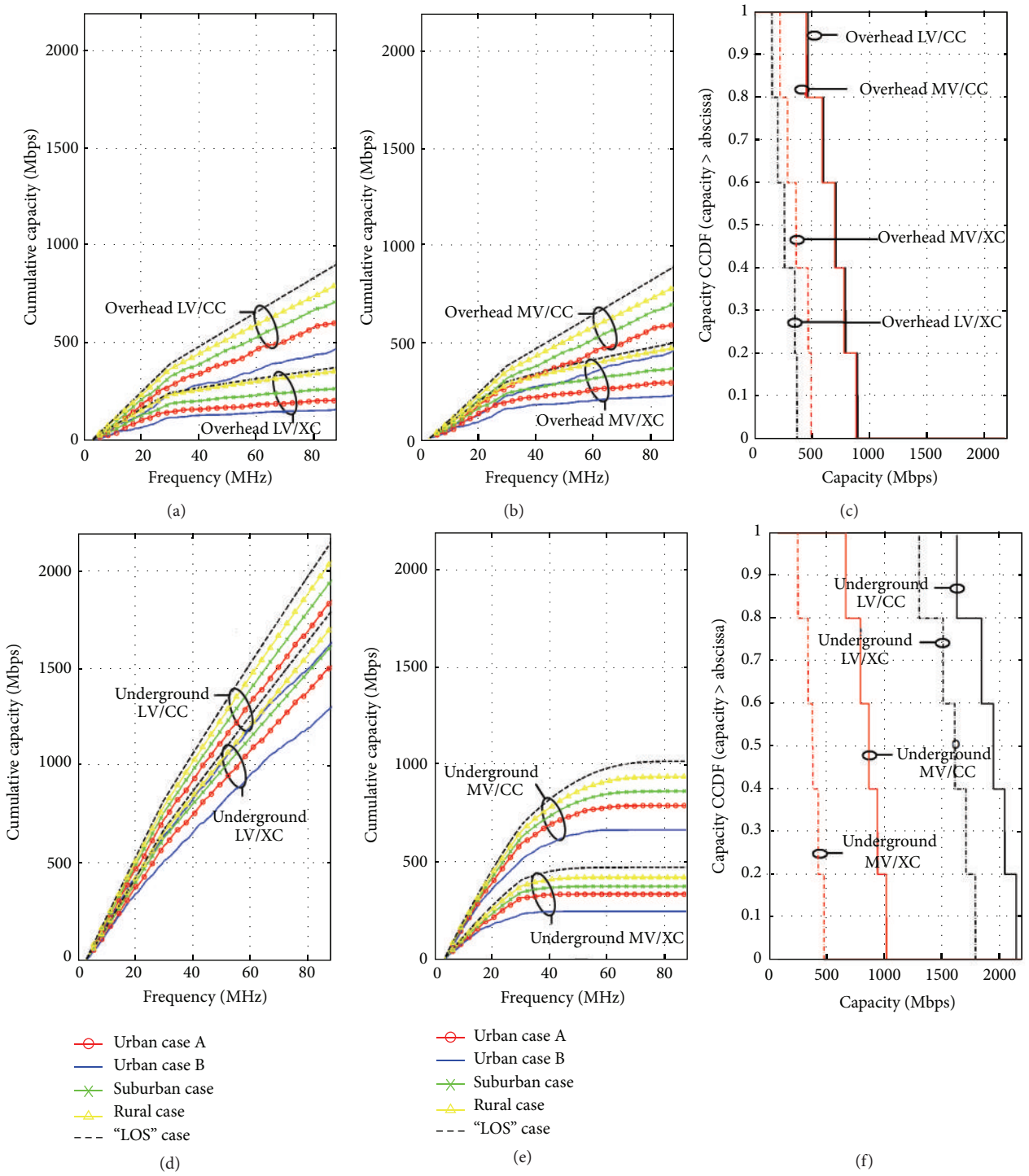

Figure 8: SISO capacity characteristics of the MIMO systems for the aforementioned indicative overhead and underground LV/BPL and MV/BPL topologies. (a), (b) SISO cumulative capacity of overhead LV/BPL and MV/BPL systems, respectively. (c) SISO capacity CCDF of overhead LV/BPL and MV/BPL systems. (d), (e) SISO cumulative capacity of underground LV/BPL and MV/BPL systems, respectively. (f) SISO capacity CCDF of underground LV/BPL and MV/BPL systems.

aforementioned indicative overhead LV/BPL topologies are plotted with respect to frequency. In Figures 9(b), 9(d), and 9(f), the 1×3 SIMO cumulative capacity, the 3×1 MISO capacity, and the 3×3 MIMO capacity, respectively, for the aforementioned indicative overhead MV/BPL topologies are displayed with respect to frequency. In Figure 9(g), the SISO/CC capacity CCDF, the SISO/XC capacity CCDF, the 1×4 SIMO capacity CCDF, the 4×1 MISO capacity CCDF,

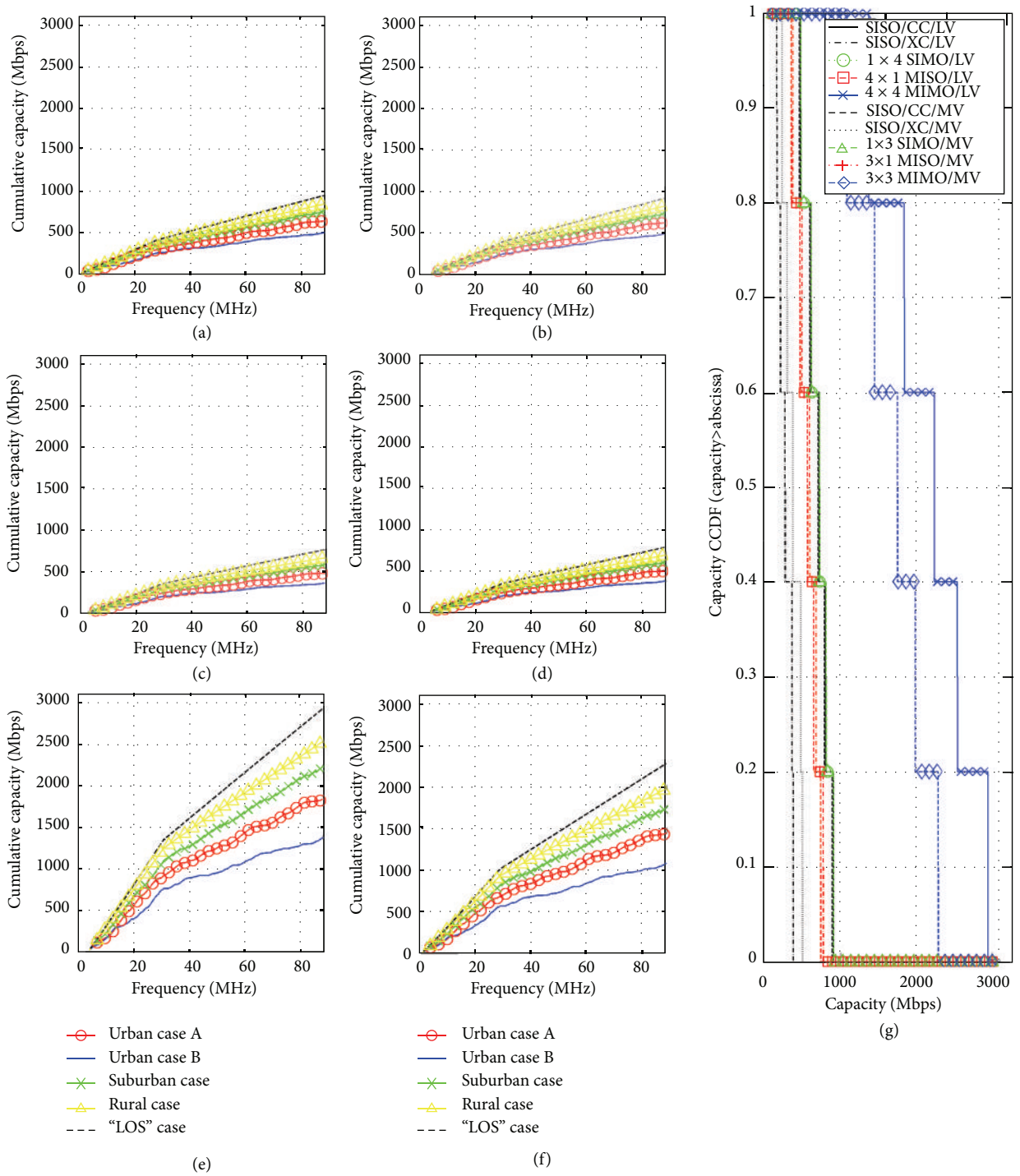

Figure 9: Capacity characteristics of various pure scheme configurations for the aforementioned indicative overhead LV/BPL and MV/BPL topologies. (a) 1 × 4 SIMO/LV cumulative capacity. (b) 1 × 3 SIMO/MV cumulative capacity. (c) 4 × 1 MISO/LV cumulative capacity. (d) 3 × 1 MISO/MV cumulative capacity. (e) 4 × 4 MIMO/LV cumulative capacity. (f) 3 × 3 MIMO/MV cumulative capacity. (g) SISO/CC/LV, SISO/XC/LV, 1 × 4 SIMO/LV, 4 × 1 MISO/LV, 4 × 4 MIMO/LV, SISO/CC/MV, SISO/XC/MV, 1 × 3 SIMO/MV, 3 × 1 MISO/MV, and 3 × 3 MIMO/MV capacity CCDF of overhead BPL systems [13, 14].

and the 4 × 4 MIMO capacity CCDF in the case of overhead LV/BPL systems for the aforementioned indicative topologies are also given. Finally, in Figure 9(g), the SISO/CC capacity CCDF, the SISO/XC capacity CCDF, the 1 × 3 SIMO capacity CCDF, the 3 × 1 MISO capacity CCDF, and the 3 × 3 MIMO capacity CCDF in the case of overhead MV/BPL systems for the aforementioned indicative topologies are also plotted. In Figures 10(a)–10(g), the respective plots in the case of underground LV/BPL and MV/BPL systems are drawn.

From the previous figures, several interesting conclusions may be drawn concerning the pure scheme configurations.

(i) As it concerns SIMO and MISO systems—1 × 4 SIMO/LV, 4 × 1 MISO/LV, 1 × 3 SIMO/MV, and 3 × 1 MISO/MV BPL systems—increasing the number of receive and transmit ports only results in a logarithmic increase in average capacity validating the above capacity analysis. In the case of full $n \times n$ MIMO/BPL systems—that is, 4 × 4 MIMO/LV and 3 × 3 MIMO/MV BPL systems—there is the capacity multiplication effect due to the $\log_2\{\cdot\}$ presence in the sum of SVD modal capacities confirming the results of MIMO capacity analysis—see (17) [41, 42, 56]. Thus, the MIMO/BPL systems offer a linear (in $\min\{n_R, n_T\}$) increase in channel capacity for no additional power or bandwidth expenditure [39, 44–46].

(ii) The full $n \times n$ MIMO/MV/BPL systems notably improve the average BPL system capacity. In all the cases, there is a significant increase of $n \times n$ MIMO system capacities compared to the respective SISO/CC ones. Analytically, in overhead BPL systems examined, the 4 × 4 MIMO/LV and 3 × 3 MIMO/MV cumulative capacities are equal to 2943 Mbps and 2288 Mbps, respectively, when the respective SISO/CC BPL system capacities are equal to 905 Mbps and 892 Mbps, respectively. In underground BPL systems, the maximum 4 × 4 MIMO/LV and 3 × 3 MIMO/MV capacities are equal to 7926 Mbps and 2736 Mbps, respectively, when the respective SISO/CC BPL system capacities are equal to 2152 Mbps and 939 Mbps, respectively. Furthermore, observing Figures 9(g) and 10(g), the MIMO/GC remains almost the same over the frequency band 3–88 MHz—denoted as GC inertia [48]. Consequently, the capacities of the 4 × 4 MIMO/LV and 3 × 3 MIMO/MV BPL systems regardless of the power grid type range by approximate GC of 3.5 and 2.7, respectively, in comparison with respective SISO/CC system capacities. The MIMO/GC is most effective for low IPSDM levels as well as for channels which exhibit high "LOS" attenuation and frequency selectivity [53].

(iii) Analyzing the overhead and underground MIMO/LV/BPL and MIMO/MV/BPL capacity results of Figures 9(g) and 10(g), in the case of the overhead and underground full 4 × 4 MIMO/LV/BPL systems, the use of three extra degrees of full phasial freedom (simultaneous insertion of three active transmit and three active receive ports) achieves a GC increase in the approximate range from 2.12 to 2.65—in comparison with the respective SISO/CC systems. Similarly, in overhead and underground full 3 × 3 MIMO/MV/BPL capacity results, despite the differences in channel attenuations, IPSDM limits, and AWGN/PSDs, the two extra degrees of full phasial freedom offer a GC increase ranging approximately from 1.48 to 1.67—in comparison with the respective SISO/CC systems. Consequently, taking also into account the GC inertia, each extra degree of full phasial freedom offers an approximate frequency-stable capacity increase factor of 0.8 regardless of the power grid type and power grid topology.

(iv) If CSI is available at transmitting end, optimal power allocation to the subchannels and transmit ports is achieved by applying the water-filling (W-F) algorithm [39, 129]. W-F algorithm permits the further exploitation of MIMO/BPL capacity.

Apart from the pure scheme configurations, depending on BPL system investment budget, technoeconomic and socioeconomic characteristics, required system complexity, power grid type, power grid topology, IPSDM limits applied, frequency band assigned, and BPL intraoperability/interoperability, different multiport implementations may be applied exploiting unequal number of transmit and receive ports. This case defines the mixed scheme configuration class that is compared against pure scheme configuration class in the following analysis [48, 50, 51].

In Table 4, the minimum value, the maximum value, the mean, and the standard deviation of the cumulative capacities for the aforementioned indicative overhead and underground LV/BPL and MV/BPL topologies for various single- and multiport implementations—either pure or mixed scheme configurations—are presented. Moreover, the possible number of different circuits (NuI) per each single- or multiport implementation that has been thoroughly examined—that is, all possible combinations among transmit and receive ports for a given scheme configuration—for each overhead and underground LV/BPL and MV/BPL topology are also reported in Table 4.

In Figure 11(a), the quantile-quantile plots of the cumulative capacities of the aforementioned overhead LV/BPL and MV/BPL topologies for a representative set of pure and mixed scheme configurations (SISO/CC/LV, 1 × 4 SIMO/LV, 4 × 3 MIMO/LV, 4 × 4 MIMO/LV, SISO/CC/MV, 1 × 3 SIMO/MV, 3 × 2 MIMO/MV, and 3 × 3 MIMO/MV) are depicted in order to test the normality of the cumulative capacity distribution functions. In these plots, the sample quantiles of cumulative capacities are displayed versus theoretical quantiles from normal distribution. In Figure 11(b), the cumulative capacity CDF of the considered pure and mixed scheme configurations (dashed lines) for the overhead LV/BPL and MV/BPL topologies is plotted. Eight CDF curves of eight random variables normally distributed with mean and standard deviation reported in Table 4 (SISO/CC/LV, 1 × 4 SIMO/LV, 4 × 3 MIMO/LV, 4 × 4 MIMO/LV, SISO/CC/MV, 1 × 3 SIMO/MV, 3 × 2 MIMO/MV, and 3 × 3 MIMO/MV, resp.) are also displayed (bold lines). In Figures 11(c) and 11(d), similar plots

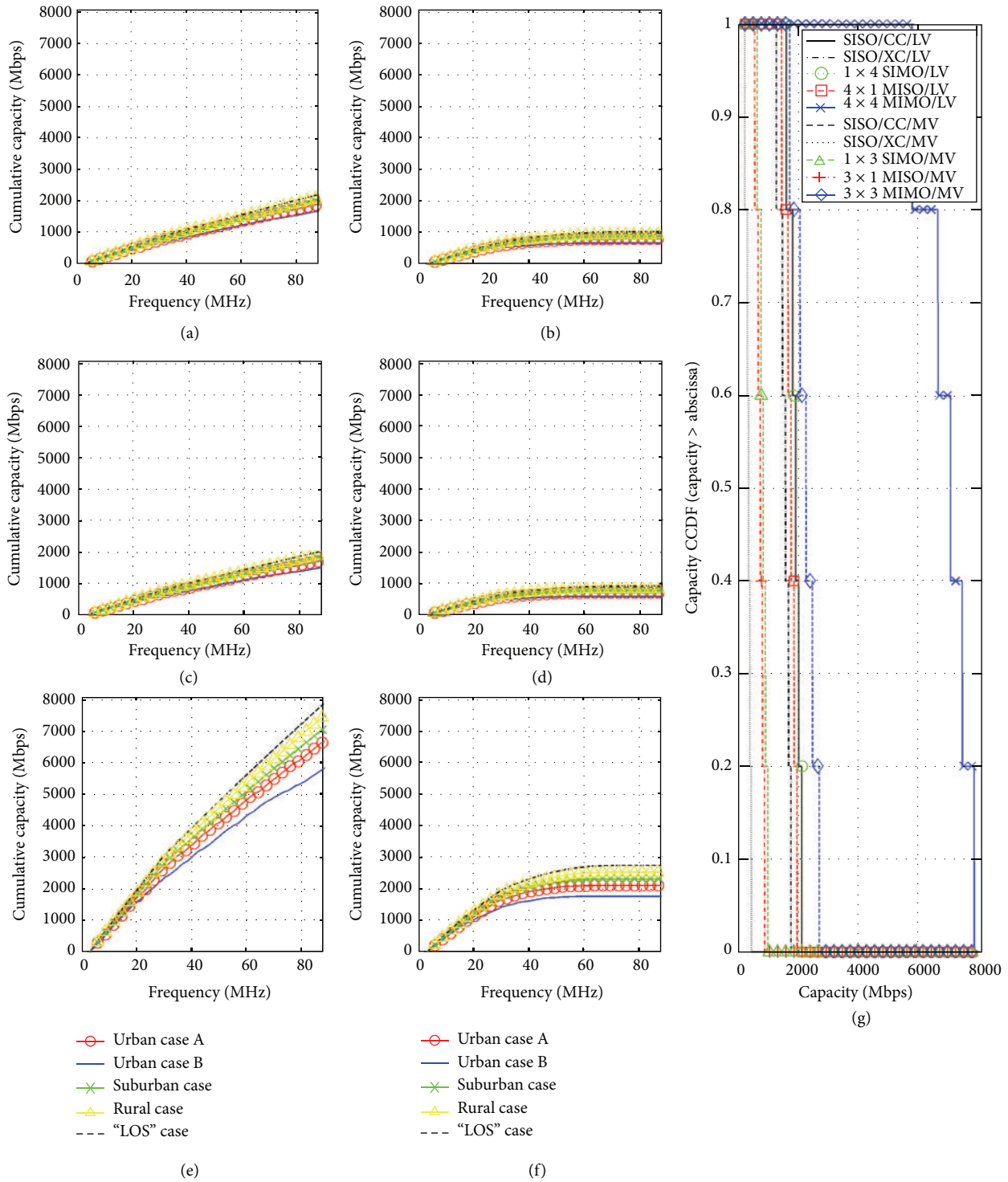

Figure 10: Capacity characteristics of various pure scheme configurations for the aforementioned indicative underground LV/BPL and MV/BPL topologies. (a) 1 × 4 SIMO/LV cumulative capacity. (b) 1 × 3 SIMO/MV cumulative capacity. (c) 4 × 1 MISO/LV cumulative capacity. (d) 3 × 1 MISO/MV cumulative capacity. (e) 4 × 4 MIMO/LV cumulative capacity. (f) 3 × 3 MIMO/MV cumulative capacity. (g) SISO/CC/LV, SISO/XC/LV, 1 × 4 SIMO/LV, 4 × 1 MISO/LV, 4 × 4 MIMO/LV, SISO/CC/MV, SISO/XC/MV, 1 × 3 SIMO/MV, 3 × 1 MISO/MV, and 3 × 3 MIMO/MV capacity CCDF of underground BPL systems [13, 14].

Table 4: Cumulative capacity and NuI for various overhead and underground MIMO/LV/BPL and MIMO/MV/BPL systems and single- and multiport scheme configurations.

	Cumulative capacity (Mbps)								NuI
	Min		Max		Mean		Standard deviation		
	OV	UN	OV	UN	OV	UN	OV	UN	
SISO/CC									
LV	471	1634	904	2152	**700**	**1928**	**168**	**200**	4
MV	459	664	892	1019	**688**	**855**	**168**	**137**	3
1 × 2 SIMO									
LV	345	1497	693	1999	**530**	**1785**	**140**	**194**	24
MV	375	471	744	769	**572**	**632**	**149**	**114**	9
1 × 3 SIMO									
LV	476	1646	907	2161	**704**	**1938**	**168**	**198**	16
MV	477	664	906	1019	**705**	**855**	**168**	**137**	3
1 × 4 SIMO									
LV	479	1655	910	2168	**707**	**1947**	**168**	**198**	4
MV	—	—	—	—	—	—	—	—	—
2 × 1 MISO									
LV	286	1397	604	1896	**453**	**1684**	**128**	**193**	24
MV	399	613	813	951	**616**	**794**	**161**	**1303**	9
3 × 1 MISO									
LV	370	1511	772	2026	**579**	**1804**	**156**	**198**	16
MV	370	583	770	912	**579**	**760**	**156**	**127**	3
4 × 1 MISO									
LV	348	1485	739	1998	**552**	**1777**	**152**	**198**	4
MV	—	—	—	—	—	—	—	—	—
2 × 2 MIMO									
LV	537	2770	1114	3779	**854**	**3349**	**241**	**390**	36
MV	602	828	1261	1381	**949**	**1129**	**264**	**212**	9
2 × 3 MIMO									
LV	536	2770	1137	3779	**851**	**3349**	**240**	**390**	24
MV	736	1166	1538	1825	**1155**	**1520**	**312**	**253**	3
2 × 4 MIMO									
LV	694	2957	1479	3987	**1102**	**3542**	**305**	**397**	6
MV	—	—	—	—	—	—	—	—	—
3 × 2 MIMO									
LV	530	2770	1135	3779	**847**	**3349**	**243**	**390**	24
MV	732	1166	1535	1824	**1151**	**1520**	**312**	**253**	3
3 × 3 MIMO									
LV	774	3058	1591	4092	**1201**	**3645**	**317**	**398**	16
MV	1082	1750	2288	2736	**1710**	**2280**	**468**	**380**	1
3 × 4 MIMO									
LV	739	3013	1543	4047	**1158**	**3601**	**312**	**3977**	4
MV	—	—	—	—	—	—	—	—	—

Table 4: Continued.

	Cumulative capacity (Mbps)								NuI
	Min		Max		Mean		Standard deviation		
	OV	UN	OV	UN	OV	UN	OV	UN	
4 × 2 MIMO									
LV	540	2770	1147	3779	**859**	**3349**	**243**	**390**	6
MV	—	—	—	—	—	—	—	—	—
4 × 3 MIMO									
LV	774	3058	1591	4092	**1201**	**3645**	**317**	**398**	4
MV	—	—	—	—	—	—	—	—	—
4 × 4 MIMO									
LV	1372	5853	2943	7926	**2187**	**7030**	**609**	**798**	1
MV	—	—	—	—	—	—	—	—	—

OV: overhead, UN: underground

are drawn in the case of underground MIMO/LV/BPL and MIMO/MV/BPL systems.

5.6. GC Analysis. To investigate further the GC potential of various single- and multiport implementations, all possible pure and mixed scheme configurations are studied and compared by means of GC assuming the median value of the aforementioned indicative topologies for each overhead and underground MIMO/LV/BPL and MIMO/MV/BPL system. In Figures 12(a) and 12(b), the GC is contour plotted with respect to the active transmit and receive ports for the overhead MIMO/LV/BPL and MIMO/MV/BPL systems, respectively. This contour plot displays GC isolines of the occurring pure and mixed scheme configurations. In Figures 12(c) and 12(d), similar plots are displayed in the case of underground LV/BPL and MV/BPL systems, respectively.

From Table 4, Figures 11(a)–11(d), and Figures 12(a)–12(d), several interesting conclusions may be deduced.

(i) The cumulative capacities of pure and mixed scheme configurations of overhead and underground LV/BPL and MV/BPL systems follow normal distributions, since the simulation plots are close to linear ones—see bold lines in Figures 11(a) and 11(c)—regardless of the scheme configuration and the power grid topology considered [4, 71–73, 78]. Meanwhile, similar to the cases of ACG and RMS-DS, suitable lognormal distributions for each overhead and underground LV/BPL and MV/BPL pure and mixed scheme configurations have been derived by appropriately fitting the simulation results. In all the cases, the proposed lognormal distributions are in excellent agreement with simulation results providing an evaluation tool of the imminent statistical channel models [71–79].

(ii) Compared to the respective SISO/CC capacities, GC of pure and mixed scheme configurations is considered to be dependent on two components: the array gain at the receiving end that corresponds to the gain in the average power of the signal combination on receive ports and the diversity gain that corresponds to the gain from increasing the system dimensionality (rank of $\mathbf{H}^{+}\{\cdot\}$). It should be noted that diversity gain mainly depends on phasial correlation between signals which are expressed by the correlation between H_{ij}^{+}, $i \in N_T$, $j \in N_R$ [130–133].

(iii) In the majority of pure and mixed scheme configurations examined, there is a significant increase of the capacity compared to SISO/CC configurations. However, apart from the factors that have already been mentioned, GC varies for different transmit and receive port combinations when a scheme configuration is given, depending on the path specific attenuation—that is, the number of CCs and XCs included in the given MIMO scheme configuration—and the correlation between the different paths. Consequently, when NuI of a scheme configuration is dominated by XCs—for example, 1 × 2 SIMO, 1 × 3 SIMO, 1 × 4 SIMO, and 2 × 1 MISO scheme configurations for overhead and underground LV/BPL systems and 1 × 2 SIMO, 1 × 3 SIMO, and 2 × 1 MISO scheme configurations for overhead and underground MV/BPL systems—the cumulative capacity and GC of these multiport implementations are lower compared to the respective values of SISO/CC ones. Contrary to the above, the remaining scheme configurations are less affected primarily due to the extra degrees of—either full or partial—phasial freedom and secondarily due to the vast presence of CCs during their implementations.

(iv) The effect of transmit and receive port increase of SIMO, MISO, and MIMO systems on the capacity is concretely highlighted in Figures 11(a)–11(d) and Figures 12(a)–12(d). As expected in the cases of equal diversity order, due to the array gain, the increase of receive ports with constant transmit ports is more efficient regarding the resulting increase in capacity than the increase in transmit ports with constant receive ports. Anyway, for a given equal diversity order, the full exploitation of MIMO technology

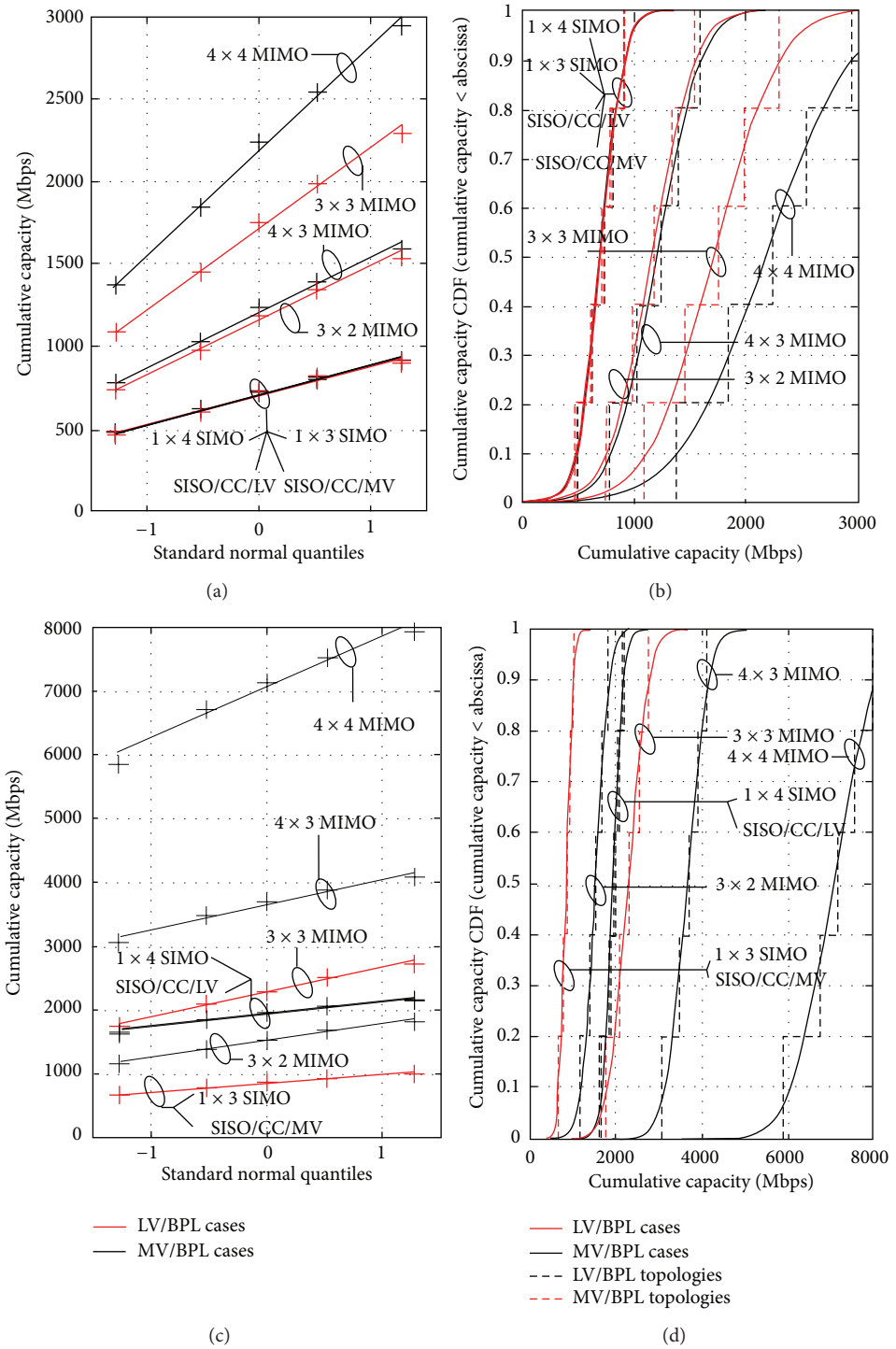

Figure 11: (a) Quantile-quantile plots of cumulative capacities of overhead LV/BPL (+) and MV/BPL (+) systems compared to theoretical normal distribution lines of the respective overhead LV/BPL and MV/BPL cases for representative pure and mixed scheme configurations. (b) Cumulative capacity CDF curves of overhead LV/BPL and MV/BPL topologies compared to theoretical normal distribution lines of the respective overhead LV/BPL and MV/BPL pure and mixed scheme configurations. (c), (d) Similar plots in underground BPL cases.

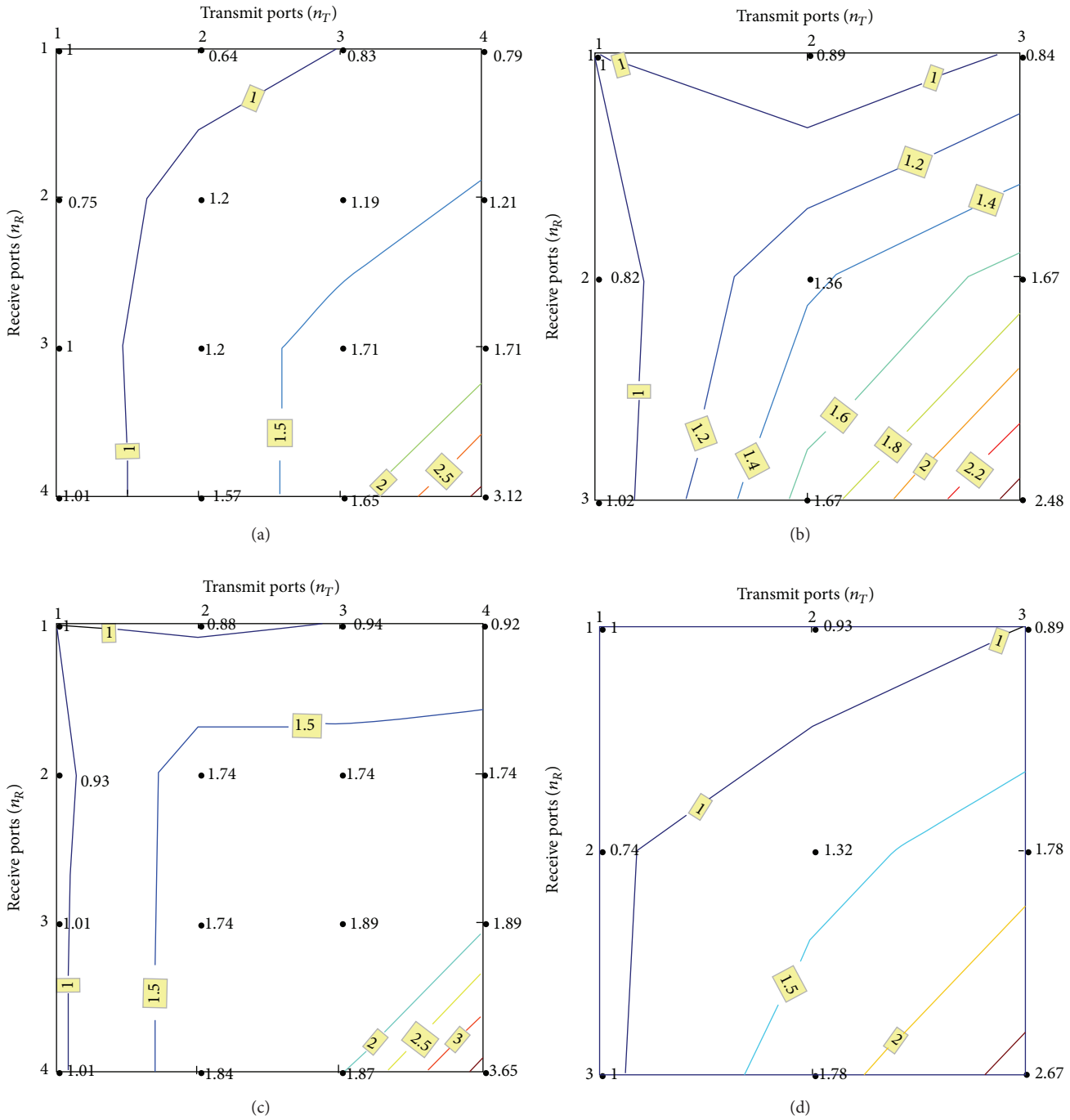

FIGURE 12: GC contour plot for various pure and mixed scheme configurations. (a) Overhead LV/BPL. (b) Overhead MV/BPL. (c) Underground LV/BPL. (d) Underground MV/BPL.

potential is achieved when transmit and receive ports are equal—that is, via the full MIMO scheme configuration deployment—validating the aforementioned approximate GC increase by 0.8 per each extra degree of full phasial freedom regardless of the power grid type and power grid topology. However, there is a significant trade-off that occurs between capacity and system implementation complexity [28, 43, 46, 130, 134].

(v) If CSI is available at transmitting end, except for the already mentioned optimal power allocation through W-F algorithm [39, 129, 130], from the point of view of fading reduction, $n_T \times n_R$ and $n_R \times n_T$ MIMO/BPL configurations present similar spectral behavior.

Therefore, the limit of MIMO capacity tends to be the same for $n_T \times n_R$ and $n_R \times n_T$ MIMO/BPL configurations [130].

(vi) Through the aforementioned significant boost of channel capacity via MIMO technology, many broadband technologies may rely on, mainly, underground MIMO/LV/BPL networked information systems so as to deliver a variety of modern broadband services such as high-speed internet, digital and HD television, and digital phone. Consequently, the overarching theme of this backbone emersion is a creation of an urban interconnected information network that permits the further urban backbone convergence between BPL and other well-established backbone communications technologies (e.g., FTTB technology) [28, 135].

(vii) Concluding this review paper of MIMO/BPL technology, it should be noted that, until now, due to different interests regarding BPL technologies—either indoor or overhead or underground, either LV or MV or HV—the BPL system implementations and standardization pursue parallel paths to their development. The varying paces of BPL technology implementation have resulted in a polyglot of capabilities that, while different, must still coexist among them and with other already established technologies [38, 128, 136]. This coexistence potential becomes requisite as imminent SG will be supported by a heterogeneous set of networking technologies. Since no single solution fits all scenarios, overhead and underground LV/BPL and MV/BPL systems need to work in a compatible way (intraoperate) before BPL technology interoperates with other broadband technologies, such as wired (e.g., fiber and DSL) and wireless (e.g., Wi-Fi and WiMAX). Compatible frequencies, equipment and signaling, green technology aspects, adequate IPSDM levels, area coverage, scalable capacity, MIMO scheme configurations, and evolution of coexistence standards must be ensured, taking the specific features of overhead and underground LV/BPL and MV/BPL systems into account [13–19, 38, 137–140].

6. Conclusions

This review paper has focused on the broadband transmission characteristics, the statistical performance metrics, and the capacity measures of overhead and underground MIMO/LV/BPL and MIMO/MV/BPL distribution power grids.

As it concerns the broadband transmission characteristics of overhead and underground LV/BPL and MV/BPL distribution networks, the well-known hybrid model has been extended through UVD modal analysis expansion pack in order to better cover the new MIMO features. The broadband transmission capabilities of such networks depend on the frequency, the power grid type, the MIMO scheme configuration, physical properties of the MTL configuration used, the end-to-end—"LOS"—distance, and the number, the electrical length, and the terminations of the branches along the end-to-end BPL signal propagation.

The investigation of the statistical performance metrics of overhead and underground MIMO/LV/BPL and MIMO/MV/BPL channels has revealed several fundamental properties that characterize various wireline channels, namely, (i) the lognormal distribution of ACG, RMS-DS, and cumulative capacity; (ii) the negative correlation between RMS-DS and ACG; and (iii) the hyperbolic correlation between RMS-DS and CB. Moreover, the existing portfolio of regression approaches has been enriched by the insertion of many regression approaches suitable for overhead and underground MIMO/LV/BPL and MIMO/MV/BPL channels in the fields of (a) RMS-DS/ACG correlation; (b) RMS-DS/CB correlation; and (c) cumulative capacity versus various single- and multiport scheme configurations.

Finally, based on the capacity metrics, the incredible capacity characteristics of overhead and underground MIMO/LV/BPL and MIMO/MV/BPL systems have been underlined. More specifically, depending on BPL system investment budget, technoeconomic and socioeconomic characteristics, required system complexity, power grid type, power grid topology, IPSDM limits applied, frequency band assigned, and BPL intraoperability/interoperability potential, different pure and mixed MIMO scheme configurations can adaptively be applied improving the today's best SISO/BPL system capacities by a factor of up to 3.65. This permits the deployment of BPL system capacities up to 8 Gbps. This capacity breakthrough transforms the existing overhead and underground LV/BPL and MV/BPL distribution networks to a *quasi*-fiber-optic backbone network, an alternative to the FTTB technology. These capacity characteristics determine the deployment of modern broadband applications, the performance of various SG applications, and the BPL system convergence in the oncoming SG network.

References

[1] T. A. Papadopoulos, C. G. Kaloudas, A. I. Chrysochos, and G. K. Papagiannis, "Application of narrowband power-line communication in medium-voltage smart distribution grids," *IEEE Transactions on Power Delivery*, vol. 28, no. 2, pp. 981–988, 2013.

[2] A. G. Lazaropoulos, "Review and progress towards the capacity boost of overhead and underground medium-voltage and low-voltage broadband over power lines networks: cooperative communications through two- and three-hop repeater systems," *ISRN Electronics*, vol. 2013, Article ID 472190, 19 pages, 2013.

[3] A. G. Lazaropoulos, "Review and progress towards the common broadband management of high-voltage transmission grids: model expansion and comparative modal analysis," *ISRN Electronics*, vol. 2012, Article ID 935286, 18 pages, 2012.

[4] S. Galli, A. Scaglione, and Z. Wang, "For the grid and through the grid: the role of power line communications in the smart grid," *Proceedings of the IEEE*, vol. 99, no. 6, pp. 998–1027, 2011.

[5] A. G. Lazaropoulos, "Towards modal integration of overhead and underground low-voltage and medium-voltage power line communication channels in the smart grid landscape: model expansion, broadband signal transmission characteristics, and statistical performance metrics (Invited Paper)," *ISRN Signal Processing*, vol. 2012, Article ID 121628, 17 pages, 2012.

[6] A. G. Lazaropoulos, "Deployment concepts for overhead high voltage broadband over power Lines connections with two-hop repeater system: capacity countermeasures against aggravated topologies and high noise environments," *Progress in Electromagnetics Research B*, vol. 44, pp. 283–307, 2012.

[7] N. Pavlidou, A. J. Han Vinck, J. Yazdani, and B. Honary, "Power line communications: state of the art and future trends," *IEEE Communications Magazine*, vol. 41, no. 4, pp. 34–40, 2003.

[8] M. Gebhardt, F. Weinmann, and K. Dostert, "Physical and regulatory constraints for communication over the power supply grid," *IEEE Communications Magazine*, vol. 41, no. 5, pp. 84–90, 2003.

[9] A. G. Lazaropoulos, "Factors influencing broadband transmission characteristics of underground low-voltage distribution networks," *IET Communications*, vol. 6, no. 17, pp. 2886–2893, 2012.

[10] A. G. Lazaropoulos, "Towards broadband over power lines systems integration: transmission characteristics of underground low-voltage distribution power lines," *Progress in Electromagnetics Research B*, no. 39, pp. 89–114, 2012.

[11] G. Jee, R. D. Rao, and Y. Cern, "Demonstration of the technical viability of PLC systems on medium- and low-voltage lines in the United States," *IEEE Communications Magazine*, vol. 41, no. 5, pp. 108–112, 2003.

[12] A. G. Lazaropoulos, "Broadband transmission and statistical performance properties of overhead high-voltage transmission networks," *Journal of Computer Networks and Communications*, vol. 2012, Article ID 875632, 16 pages, 2012.

[13] A. G. Lazaropoulos, "Green overhead and underground multiple-input multiple-output medium voltage broadband over power lines networks: energy-efficient power control," in *Journal of Global Optimization*, vol. 2012, pp. 1–28, 2012.

[14] A. G. Lazaropoulos, "Overhead and underground MIMO low voltage broadband over power lines networks and EMI regulations: towards greener capacity performances," *Computers and Electrical Engineering*, 2013.

[15] A. G. Lazaropoulos and P. G. Cottis, "Transmission characteristics of overhead medium-voltage power-line communication channels," *IEEE Transactions on Power Delivery*, vol. 24, no. 3, pp. 1164–1173, 2009.

[16] A. G. Lazaropoulos and P. G. Cottis, "Capacity of overhead medium voltage power line communication channels," *IEEE Transactions on Power Delivery*, vol. 25, no. 2, pp. 723–733, 2010.

[17] A. G. Lazaropoulos and P. G. Cottis, "Broadband transmission via underground medium-voltage power lines. Part I: transmission characteristics," *IEEE Transactions on Power Delivery*, vol. 25, no. 4, pp. 2414–2424, 2010.

[18] A. G. Lazaropoulos and P. G. Cottis, "Broadband transmission via underground medium-voltage power lines. Part II: capacity," *IEEE Transactions on Power Delivery*, vol. 25, no. 4, pp. 2425–2434, 2010.

[19] A. G. Lazaropoulos, "Broadband transmission characteristics of overhead high-voltage power line communication channels," *Progress In Electromagnetics Research B*, no. 36, pp. 373–398, 2011.

[20] P. S. Henry, "Interference characteristics of broadband power line communication systems using aerial medium voltage wires," *IEEE Communications Magazine*, vol. 43, no. 4, pp. 92–98, 2005.

[21] S. Liu and L. J. Greenstein, "Emission characteristics and interference constraint of overhead medium-voltage Broadband Power Line (BPL) systems," in *Proceedings of the IEEE Global Telecommunications Conference (GLOBECOM '08)*, pp. 2921–2925, New Orleans, La, USA, December 2008.

[22] D. Fenton and P. Brown, "Modelling cumulative high frequency radiated interference from power line communication systems," in *Proceedings of the IEEE International Conference on Power Line Communications and Its Applications*, Athens, Greece, March 2002.

[23] M. Götz, M. Rapp, and K. Dostert, "Power line channel characteristics and their effect on communication system design," *IEEE Communications Magazine*, vol. 42, no. 4, pp. 78–86, 2004.

[24] M. Zimmermann and K. Dostert, "A multipath model for the powerline channel," *IEEE Transactions on Communications*, vol. 50, no. 4, pp. 553–559, 2002.

[25] L. Lampe, R. Schober, and S. Yiu, "Distributed space-time coding for multihop transmission in power line communication networks," *IEEE Journal on Selected Areas in Communications*, vol. 24, no. 7, pp. 1389–1400, 2006.

[26] A. S. Ibrahim, A. K. Sadek, S. Weifeng, and K. J. R. Liu, "Cooperative communications with relay-selection: when to cooperate and whom to cooperate with?" *IEEE Transactions on Wireless Communications*, vol. 7, no. 7, pp. 2814–2827, 2008.

[27] A. Nosratinia, T. E. Hunter, and A. Hedayat, "Cooperative communication in wireless networks," *IEEE Communications Magazine*, vol. 42, no. 10, pp. 74–80, 2004.

[28] L. Wang and L. Hanzo, "Dispensing with channel estimation: differentially modulated cooperative wireless communications," *IEEE Communications Surveys and Tutorials*, vol. 14, no. 3, pp. 836–857, 2012.

[29] Y.-W. Hong, W.-J. Huang, F.-H. Chiu, and C.-C. J. Kuo, "Cooperative communications in resource-constrained wireless networks," *IEEE Signal Processing Magazine*, vol. 24, no. 3, pp. 47–57, 2007.

[30] M. Gastpar, "On capacity under receive and spatial spectrum-sharing constraints," *IEEE Transactions on Information Theory*, vol. 53, no. 2, pp. 471–487, 2007.

[31] F. Versolatto and A. M. Tonello, "An MTL theory approach for the simulation of MIMO power-line communication channels," *IEEE Transactions on Power Delivery*, vol. 26, no. 3, pp. 1710–1717, 2011.

[32] V. Oksman and S. Galli, "G.hn: the new ITU-T home networking standard," *IEEE Communications Magazine*, vol. 47, no. 10, pp. 138–145, 2009.

[33] D. Schneider, J. Speidel, L. Stadelmeier, and D. Schill, "Precoded spatial multiplexing MIMO for inhome power line Communications," in *Proceedings of the IEEE Global Telecommunications Conference (GLOBECOM '08)*, pp. 2901–2905, New Orleans, La, USA, December 2008.

[34] "OPERA2, D24: document of conclusions about the different services tested over the new generation PLC network (M24 definitive version)," IST Integrated Project 026920, 2008.

[35] N. Golmie, N. Chevrollier, and O. Rebala, "Bluetooth and WLAN coexistence: challenges and solutions," *IEEE Wireless Communications Magazine*, vol. 10, no. 6, pp. 347–357, 2003.

[36] "OPERA2, D51: white Paper: OPERA technology (final version)," IST Integrated Project 026920, 2008.

[37] M. Kuhn, S. Berger, I. Hammerström, and A. Wittneben, "Power line enhanced cooperative wireless communications," *IEEE Journal on Selected Areas in Communications*, vol. 24, no. 7, pp. 1401–1410, 2006.

[38] L. Hanzo, M. El-Hajjar, and O. Alamri, "Near-capacity wireless transceivers and cooperative communications in the MIMO Era: evolution of standards, waveform design, and future perspectives," *Proceedings of the IEEE*, vol. 99, no. 8, pp. 1343–1385, 2011.

[39] A. J. Paulraj, D. A. Gore, R. U. Nabar, and H. Bölcskei, "An overview of MIMO communications: a key to gigabit wireless," *Proceedings of the IEEE*, vol. 92, no. 2, pp. 198–217, 2004.

[40] E. Biglieri, J. Proakis, and S. Shamai, "Fading channels: information-theoretic and communications aspects," *IEEE Transactions on Information Theory*, vol. 44, no. 6, pp. 2619–2692, 1998.

[41] D. Gesbert, M. Shafi, D.-S. Shiu, P. J. Smith, and A. Naguib, "From theory to practice: an overview of MIMO space-time coded wireless systems," *IEEE Journal on Selected Areas in Communications*, vol. 21, no. 3, pp. 281–302, 2003.

[42] A. Goldsmith, S. A. Jafar, N. Jindal, and S. Vishwanath, "Capacity limits of MIMO channels," *IEEE Journal on Selected Areas in Communications*, vol. 21, no. 5, pp. 684–702, 2003.

[43] Q. Du and X. Zhang, "QoS-aware base-station selections for distributed MIMO links in broadband wireless networks," *IEEE Journal on Selected Areas in Communications*, vol. 29, no. 6, pp. 1123–1138, 2011.

[44] S. Vishwanath, N. Jindal, and A. Goldsmith, "Duality, achievable rates, and sum-rate capacity of Gaussian MIMO broadcast channels," *IEEE Transactions on Information Theory*, vol. 49, no. 10, pp. 2658–2668, 2003.

[45] G. Caire and S. Shamai, "On the achievable throughput of a multiantenna Gaussian broadcast channel," *IEEE Transactions on Information Theory*, vol. 49, no. 7, pp. 1691–1706, 2003.

[46] S. Sugiura, S. Chen, and L. Hanzo, "MIMO-aided near-capacity turbo transceivers: taxonomy and performance versus complexity," *IEEE Communications Surveys and Tutorials*, vol. 14, no. 2, pp. 421–442, 2012.

[47] M. Tlich, A. Zeddam, F. Moulin, and F. Gauthier, "Indoor power-line communications channel characterization up to 100 MHz. Part I: one-parameter deterministic model," *IEEE Transactions on Power Delivery*, vol. 23, no. 3, pp. 1392–1401, 2008.

[48] R. Hashmat, P. Pagani, A. Zeddam, and T. Chonave, "MIMO communications for inhome PLC Networks: measurements and results up to 100 MHz," in *Proceedings of the 14th Annual International Symposium on Power Line Communications and its Applications (IEEE ISPLC '10)*, pp. 120–124, Rio de Janeiro, Brazil, March 2010.

[49] A. Canova, N. Benvenuto, and P. Bisaglia, "Receivers for MIMO-PLC channels: throughput comparison," in *Proceedings of the 14th Annual International Symposium on Power Line Communications and its Applications (IEEE ISPLC '10)*, pp. 114–119, Rio de Janeiro, Brazil, March 2010.

[50] D. Schneider, A. Schwager, J. Speidel, and A. Dilly, "Implementation and results of a MIMO PLC feasibility study," in *Proceedings of the IEEE International Symposium on Power Line Communications and Its Applications (ISPLC '11)*, pp. 54–59, Udine, Italy, April 2011.

[51] M. Biagi, "MIMO self-interference mitigation effects on PLC relay networks," in *Proceedings of the IEEE International Symposium on Power Line Communications and Its Applications (ISPLC '11)*, pp. 182–186, Udine, Italy, April 2011.

[52] M. Biagi, "MIMO self-interference mitigation effects on power line relay networks," *IEEE Communications Letters*, vol. 15, no. 8, pp. 866–868, 2011.

[53] D. Schneider, J. Speidel, L. Stadelmeier, D. Schill, and A. Schwager, "Potential of MIMO for inhome power line communications," in *Proceedings of the the ITGFachtagung*, Dortmund, Germany, March 2009.

[54] A. Schwager, D. Schneider, W. Baschlin, A. Dilly, and J. Speidel, "MIMO PLC: theory, measurements and system setup," in *Proceedings of the IEEE International Symposium on Power Line Communications and Its Applications (ISPLC '11)*, pp. 48–53, Udine, Italy, April 2011.

[55] L. Stadelmeier, D. Schneider, D. Schill, A. Schwager, and J. Speidel, "MIMO for inhome power line communications," in *Proceedings of the International Conference on Source and Channel Coding*, Ulm, Germany, January 2008.

[56] F. Versolatto and A. M. Tonello, "A MIMO PLC random channel generator and capacity analysis," in *Proceedings of the IEEE International Symposium on Power Line Communications and Its Applications (ISPLC '11)*, pp. 66–71, Udine, Italy, April 2011.

[57] P. Amirshahi and M. Kavehrad, "High-frequency characteristics of overhead multiconductor power lines for broadband communications," *IEEE Journal on Selected Areas in Communications*, vol. 24, no. 7, pp. 1292–1302, 2006.

[58] T. Sartenaer, *Multiuser communications over frequency selective wired channels and applications to the powerline access network [Ph.D. thesis]*, Université catholique de Louvain, Louvain-la-Neuve, Belgium, 2004.

[59] T. Calliacoudas and F. Issa, "Multiconductor transmission lines and cables solver: an efficient simulation tool for plc channel networks development," in *Proceedings of the IEEE International Conference on Power Line Communications and Its Applications*, Athens, Greece, March 2002.

[60] C. R. Paul, *Analysis of Multiconductor Transmission Lines*, Wiley, New York, NY, USA, 1994.

[61] J. A. B. Faria, *Multiconductor Transmission-Line Structures: Modal Analysis Techniques*, Wiley, New York, NY, USA, 1994.

[62] T. Sartenaer and P. Delogne, "Deterministic modeling of the (shielded) outdoor power line channel based on the Multiconductor Transmission Line equations," *IEEE Journal on Selected Areas in Communications*, vol. 24, no. 7, pp. 1277–1290, 2006.

[63] T. Sartenaer and P. Delogne, "Powerline cables modelling for broadband communications," in *Proceedings of the IEEE International Conference on the Power Line Communications and Its Applications*, pp. 331–337, Malmö, Sweden, April 2001.

[64] S. Galli and T. C. Banwell, "A deterministic frequency-domain model for the indoor power line transfer function," *IEEE Journal on Selected Areas in Communications*, vol. 24, no. 7, pp. 1304–1315, 2006.

[65] A. Pérez, A. M. Sanchez, J. R. Regué et al., "Circuital and modal characterization of the power-line network in the PLC band," *IEEE Transactions on Power Delivery*, vol. 24, no. 3, pp. 1182–1189, 2009.

[66] K. Dostert, *Powerline Communications*, Prentice-Hall, Upper Saddle River, NJ, USA, 2001.

[67] P. Amirshahi, *Broadband access and home networking through powerline networks [Ph.D. thesis]*, Pennsylvania State University, University Park, Pa, USA, 2006.

[68] H. Meng, S. Chen, Y. L. Guan et al., "Modeling of transfer characteristics for the broadband power line communication channel," *IEEE Transactions on Power Delivery*, vol. 19, no. 3, pp. 1057–1064, 2004.

[69] S. Barmada, A. Musolino, and M. Raugi, "Innovative model for time-varying power line communication channel response

evaluation," *IEEE Journal on Selected Areas in Communications*, vol. 24, no. 7, pp. 1317–1325, 2006.

[70] M. D'Amore and M. S. Sarto, "A new formulation of lossy ground return parameters for transient analysis of multiconductor dissipative lines," *IEEE Transactions on Power Delivery*, vol. 12, no. 1, pp. 303–309, 1997.

[71] S. Galli, "A novel approach to the statistical modeling of wireline channels," *IEEE Transactions on Communications*, vol. 59, no. 5, pp. 1332–1345, 2011.

[72] S. Galli, "A simplified model for the indoor power line channel," in *Proceedings of the IEEE International Symposium on Power Line Communications and its Applications (ISPLC '09)*, pp. 13–19, Dresden, Germany, April 2009.

[73] S. Galli, "A simple two-tap statistical model for the power line channel," in *Proceedings of the 14th Annual International Symposium on Power Line Communications and its Applications (IEEE ISPLC '10)*, pp. 242–248, Rio de Janeiro, Brazil, March 2010.

[74] "ITU-T SG15/Q4, Powerline channel data," Contribution NIPP-NAI-2007-107R1, 2007.

[75] B. O'Mahony, "Field testing of high-speed power line communications in North American homes," in *Proceedings of the IEEE International Symposium on Power Line Communications and Its Applications (ISPLC '06)*, pp. 155–159, Orlando, Fla, USA, March 2006.

[76] F. Versolatto and A. M. Tonello, "Analysis of the PLC channel statistics using a bottom-up random simulator," in *Proceedings of the 14th Annual International Symposium on Power Line Communications and its Applications (IEEE ISPLC '10)*, pp. 236–241, Rio de Janeiro, Brazil, March 2010.

[77] A. M. Tonello, F. Versolatto, and C. Tornelli, "Analysis of impulsive UWB modulation on a real MV test network," in *Proceedings of the IEEE International Symposium on Power Line Communications and Its Applications (ISPLC '11)*, pp. 18–23, Udine, Italy, April 2011.

[78] M. Antoniali, A. M. Tonello, M. Lenardon, and A. Qualizza, "Measurements and analysis of PLC channels in a cruise ship," in *Proceedings of the IEEE International Symposium on Power Line Communications and Its Applications (ISPLC '11)*, pp. 102–107, Udine, Italy, April 2011.

[79] A. M. Tonello and F. Versolatto, "Bottom-up statistical PLC channel modeling: part II: inferring the statistics," *IEEE Transactions on Power Delivery*, vol. 25, no. 4, pp. 2356–2363, 2010.

[80] F. J. Cañete, J. A. Cortés, L. Díez, and J. T. Entrambasaguas, "A channel model proposal for indoor power line communications," *IEEE Communications Magazine*, vol. 49, no. 12, pp. 166–174.

[81] T. S. Rappaport, *Wireless Communications*, Prentice-Hall, Upper Saddle River, NJ, USA, 2002.

[82] M. Tlich, G. Avril, and A. Zeddam, "Coherence bandwidth and its relationship with the rms delay spread for PLC channels using measurements up to 100 MHz," in *Home Networking*, IFIP International Federation for Information Processing, pp. 129–142, 2007.

[83] "DLC+VIT4IP, D1. 2: overall system architecture design DLC system architecture," FP7 Integrated Project 247750, 2010.

[84] F. Issa, D. Chaffanjon, E. P. de la Bâthie, and A. Pacaud, "An efficient tool for modal analysis transmission lines for PLC networks development," in *Proceedings of the IEEE International Conference on Power Line Communications and Its Applications*, Athens, Greece, March 2002.

[85] J. Anatory and N. Theethayi, "On the efficacy of using ground return in the broadband power-line communications: a transmission-line analysis," *IEEE Transactions on Power Delivery*, vol. 23, no. 1, pp. 132–139, 2008.

[86] T. A. Papadopoulos, B. D. Batalas, A. Radis, and G. K. Papagiannis, "Medium voltage network PLC modeling and signal propagation analysis," in *Proceedings of the IEEE International Symposium on Power Line Communications and Its Applications (ISPLC '07)*, pp. 284–289, Pisa, Italy, March 2007.

[87] "OPERA1, D44: report presenting the architecture of plc system, the electricity network topologies, the operating modes and the equipment over which PLC access system will be installed," IST Integrated Project 507667, 2005.

[88] M. Tang and M. Zhai, "Research of transmission parameters of four-conductor cables for power line communication," in *Proceedings of the International Conference on Computer Science and Software Engineering (CSSE '08)*, pp. 1306–1309, Wuhan, China, December 2008.

[89] M. D'Amore and M. S. Sarto, "Simulation models of a dissipative transmission line above a lossy ground for a wide-frequency range. Part I: single conductor configuration," *IEEE Transactions on Electromagnetic Compatibility*, vol. 38, no. 2, pp. 127–138, 1996.

[90] M. D. 'Amore and M. S. Sarto, "Simulation models of a dissipative transmission line above a lossy ground for a wide-frequency range. Part II: multi-conductor configuration," *IEEE Transactions on Electromagnetic Compatibility*, vol. 38, no. 2, pp. 139–149, 1996.

[91] P. C. J. M. van der Wielen, *On-line detection and location of partial discharges in medium-voltage power cables [Ph.D. thesis]*, Eindhoven University of Technology, Eindhoven, the Netherlands, 2005.

[92] "OPERA1, D5: pathloss as a function of frequency, distance and network topology for various LV and MV European powerline networks," IST Integrated Project 507667, 2005.

[93] P. C. J. M. van der Wielen, E. F. Steennis, and P. A. A. F. Wouters, "Fundamental aspects of excitation and propagation of on-line partial discharge signals in three-phase medium voltage cable systems," *IEEE Transactions on Dielectrics and Electrical Insulation*, vol. 10, no. 4, pp. 678–688, 2003.

[94] J. Veen, *On-line signal analysis of partial discharges in medium-voltage power cables [Ph.D. thesis]*, Technische Universiteit Eindhoven, Eindhoven, the Netherlands, 2005.

[95] N. Theethayi, *Electromagnetic interference in distributed outdoor electrical systems, with an emphasis on lightning interaction with electrified railway network [Ph.D. thesis]*, Uppsala University, Uppsala, Sweden, 2005.

[96] E. F. Vance, *Coupling To Cable Shields*, Wiley, New York, NY, USA, 1978.

[97] R. Aquilué, *Power line communications for the electrical utility: physical layer design and channel modeling [Ph.D. thesis]*, Universitat Ramon Llull, Enginyeria I Arquitectura La Salle, Barcelona, Spain, 2008.

[98] A. Cataliotti, A. Daidone, and G. Tinè, "Power line communication in medium voltage systems: characterization of MV cables," *IEEE Transactions on Power Delivery*, vol. 23, no. 4, pp. 1896–1902, 2008.

[99] J. Anatory, N. Theethayi, R. Thottappillil, M. M. Kissaka, and N. H. Mvungi, "The influence of load impedance, line length, and branches on underground cable power-line communications (PLC) systems," *IEEE Transactions on Power Delivery*, vol. 23, no. 1, pp. 180–187, 2008.

[100] D. A. Tsiamitros, G. K. Papagiannis, and P. S. Dokopoulos, "Earth return impedances of conductor arrangements in multilayer soils. Part I: theoretical model," *IEEE Transactions on Power Delivery*, vol. 23, no. 4, pp. 2392–2400, 2008.

[101] D. A. Tsiamitros, G. K. Papagiannis, and P. S. Dokopoulos, "Earth return impedances of conductor arrangements in multilayer soils. Part II: numerical results," *IEEE Transactions on Power Delivery*, vol. 23, no. 4, pp. 2401–2408, 2008.

[102] F. Rachidi and S. V. Tkachenko, *Electromagnetic Field Interaction with Transmission Lines: From Classical Theory to HF Radiation Effects*, WIT press, Southampton, UK, 2008.

[103] J. R. Carson, "Wave propagation in overhead wires with ground return," *Bell System Technical Journal*, vol. 5, pp. 539–554, 1926.

[104] H. Kikuchi, "Wave propagation along an infinite wire above ground at high frequencies," *Electrotechnical Journal of Japan*, vol. 2, pp. 73–78, 1956.

[105] H. Kikuchi, "On the transition form a ground return circuit to a surface waveguide," in *Proceedings of the Congress on Ultrahigh Frequency Circuits Antennas*, pp. 39–45, Paris, France, October 1957.

[106] S. Galli and T. Banwell, "A novel approach to the modeling of the indoor power line channel. Part II: transfer function and its properties," *IEEE Transactions on Power Delivery*, vol. 20, no. 3, pp. 1869–1878, 2005.

[107] B. S. Yarman and A. Fettweis, "Computer-aided double matching via parametric representation of Brune functions," *IEEE Transactions on Circuits and Systems*, vol. 37, no. 2, pp. 212–222, 1990.

[108] R. Araneo, S. Celozzi, G. Lovat, and F. Maradei, "Multi-port impedance matching technique for power line communications," in *Proceedings of the IEEE International Symposium on Power Line Communications and Its Applications (ISPLC '11)*, pp. 96–101, Udine, Italy, April 2011.

[109] L. H.-J. Lampe and J. B. Huber, "Bandwidth efficient power line communications based on OFDM," *AEU-Archiv fur Elektronik und Ubertragungstechnik*, vol. 54, no. 1, pp. 2–12, 2000.

[110] M. Crussière, J. Y. Baudais, and J. F. Hélard, "Adaptive spread spectrum multicarrier multiple-access over wirelines," *IEEE Journal on Selected Areas in Communications*, vol. 24, no. 7, pp. 1377–1388, 2006.

[111] P. Achaichia, M. Le Bot, and P. Siohan, "OFDM/OQAM: a solution to efficiently increase the capacity of future PLC networks," *IEEE Transactions on Power Delivery*, vol. 26, no. 4, pp. 2443–2455, 2011.

[112] Y.-H. Kim and J.-H. Lee, "Comparison of passband and baseband transmission schemes for power-line communication OFDM systems," *IEEE Transactions on Power Delivery*, vol. 26, no. 4, pp. 2466–2475, 2011.

[113] J. Anatory, N. Theethayi, R. Thottappillil, M. Kissaka, and N. Mvungi, "The effects of load impedance, line length, and branches in typical low-voltage channels of the BPLC systems of developing countries: transmission-line analyses," *IEEE Transactions on Power Delivery*, vol. 24, no. 2, pp. 621–629, 2009.

[114] J. Anatory, N. Theethayi, and R. Thottappillil, "Power-line communication channel model for interconnected networks. Part II: multiconductor system," *IEEE Transactions on Power Delivery*, vol. 24, no. 1, pp. 124–128, 2009.

[115] J. Song, C. Pan, Q. Wu et al., "Field trial of digital video transmission over medium-voltage powerline with time-domain synchronous orthogonal frequency division multiplexing technology," in *Proceedings of the International Symposium on Power Line Communications and Its Applications (ISPLC '07)*, pp. 559–564, Pisa, Italy, March 2007.

[116] R. Aquilué, M. Ribó, J. R. Regué, J. L. Pijoan, and G. Sánchez, "Scattering parameters-based channel characterization and modeling for underground medium-voltage power-line communications," *IEEE Transactions on Power Delivery*, vol. 24, no. 3, pp. 1122–1131, 2009.

[117] H. Liu, J. Song, B. Zhao, and X. Li, "Channel study for medium-voltage power network," in *Proceedings of the IEEE International Symposium on Power Line Communications and Its Applications (ISPLC '06)*, pp. 245–250, Orlando, Fla, USA, March 2006.

[118] Ofcom, "DS2 PLT Measurements in Crieff," Tech. Rep. 793 (Part 2), Ofcom, 2005, http://www.ofcom.org.uk/research/technology/research/archive/cet/powerline/ds2.pdf.

[119] Ofcom, "Ascom PLT Measurements in Winchester," Tech. Rep. 793 (Part 1), Ofcom, 2005.

[120] P. A. A. F. Wouters, P. C. J. M. van der Wielen, J. Veen, P. Wagenaars, and E. F. Wagenaars, "Effect of cable load impedance on coupling schemes for MV power line communication," *IEEE Transactions on Power Delivery*, vol. 20, no. 2, pp. 638–645, 2005.

[121] A. Cataliotti, V. Cosentino, D. Di Cara, and G. Tiné, "Simulation and laboratory experimental tests of a line to shield medium-voltage power-line communication system," *IEEE Transactions on Power Delivery*, vol. 26, no. 4, pp. 2829–2836, 2011.

[122] M. Tlich, A. Zeddam, F. Moulin, and F. Gauthier, "Indoor power-line communications channel characterization up to 100 MHz. Part II: time-frequency analysis," *IEEE Transactions on Power Delivery*, vol. 23, no. 3, pp. 1402–1409, 2008.

[123] Nexans deutschland industries GmbH and Co. KG: catalogue LV underground power cables distribution cables, 2011.

[124] Tele-Fonika Kable GmbH, Cables and wires, 2008.

[125] G. J. Anders, *Rating of Electric Power Cables*, IEEE Press, New York, NY, USA, 1997.

[126] D. Veronesi, R. Riva, P. Bisaglia et al., "Characterization of in-home MIMO power line channels," in *Proceedings of the IEEE International Symposium on Power Line Communications and Its Applications (ISPLC '11)*, pp. 42–47, Udine, Italy, April 2011.

[127] W. Q. Malik, "MIMO capacity convergence in frequency-selective channels," *IEEE Transactions on Communications*, vol. 57, no. 2, pp. 353–356, 2009.

[128] K. Peppas, F. Lazarakis, C. Skianis, A. A. Alexandridis, and K. Dangakis, "Impact of MIMO techniques on the interoperability between UMTS-HSDPA and WLAN wireless systems," *IEEE Communications Surveys and Tutorials*, vol. 13, no. 4, pp. 708–720, 2011.

[129] R. G. Gallager, *Information Theory and Reliable Communication*, Wiley, New York, NY, USA, 1968.

[130] M. A. Khalighi, K. Raoof, and G. Jourdain, "Capacity of wireless communication systems employing antenna arrays, a tutorial study," *Wireless Personal Communications*, vol. 23, no. 3, pp. 321–352, 2002.

[131] J. B. Andersen, "Array gain and capacity for known random channels with multiple element arrays at both ends," *IEEE Journal on Selected Areas in Communications*, vol. 18, no. 11, pp. 2172–2178, 2000.

[132] P.-S. Kildal and K. Rosengren, "Correlation and capacity of MIMO systems and mutual coupling, radiation efficiency, and diversity gain of their antennas: simulations and measurements in a reverberation chamber," *IEEE Communications Magazine*, vol. 42, no. 12, pp. 104–112, 2004.

[133] K. Sulonen, P. Suvikunnas, L. Vuokko, J. Kivinen, and P. Vainikainen, "Comparison of MIMO antenna configurations in picocell and microcell environments," *IEEE Journal on Selected Areas in Communications*, vol. 21, no. 5, pp. 703–712, 2003.

[134] Y. J. Zhang and A. M.-C. So, "Optimal spectrum sharing in MIMO cognitive radio networks via semidefinite programming," *IEEE Journal on Selected Areas in Communications*, vol. 29, no. 2, pp. 362–373, 2011.

[135] O. Tipmongkolsilp, S. Zaghloul, and A. Jukan, "The evolution of cellular backhaul technologies: current issues and future trends," *IEEE Communications Surveys and Tutorials*, vol. 13, no. 1, pp. 97–113, 2011.

[136] P.-D. Arapoglou, K. Liolis, M. Bertinelli, A. Panagopoulos, P. Cottis, and R. de Gaudenzi, "MIMO over satellite: a review," *IEEE Communications Surveys and Tutorials*, vol. 13, no. 1, pp. 27–51, 2011.

[137] K. Hooghe and M. Guenach, "Toward green copper broadband access networks," *IEEE Communications Magazine*, vol. 49, no. 8, pp. 87–93, 2011.

[138] W. Vereecken, W. van Heddeghem, M. Deruyck et al., "Power consumption in telecommunication networks: overview and reduction strategies," *IEEE Communications Magazine*, vol. 49, no. 6, pp. 62–69, 2011.

[139] M. M. Rahman, C. S. Hong, S. Lee, J. Lee, M. A. Razzaque, and J. H. Kim, "Medium access control for power line communications: an overview of the IEEE 1901 and ITU-T G.hn standards," *IEEE Communications Magazine*, vol. 49, no. 6, pp. 183–191, 2011.

[140] R. Bolla, F. Davoli, R. Bruschi, K. Christensen, F. Cucchietti, and S. Singh, "The potential impact of green technologies in next-generation wireline networks: is there room for energy saving optimization?" *IEEE Communications Magazine*, vol. 49, no. 8, pp. 80–86, 2011.